THROUGH THE WALL IMAGING RADAR

By

Muhammad Ijlal Baig

Hafiz Ahmad Arif

Muhammad Zaeem Aslam Bajwa

Directing Staff

Dr. Naveed Iqbal Rao

Asst. Prof Zeeshan Zahid

Lab. Engr. Sara Viqar

Submitted to the Faculty of Electrical Engineering, Military College of Signals
National University of Sciences and Technology, Rawalpindi in partial fulfillment for the requirements of a B.E in Telecommunication Engineering

June 2013

CERTIFICATE OF CORRECTNESS AND APPROVAL

It is certified that work contained in this thesis titled "Through the Wall Imaging RADAR", carried out by Muhammad Ijlal Baig, Hafiz Ahmad Arif and Muhammad Zaeem Aslam Bajwa under the supervision of Dr. Naveed Iqbal Rao in partial fulfillment of Degree of Bachelor of Telecommunication Engineering, is correct and approved.

Approved by

_____

(Dr. Naveed Iqbal Rao)
Project Directing Staff (DS)
Military College of Signals (MCS)

Dated: _____ June 2013

ABSTRACT

THROUGH THE WALL IMAGING RADAR

The ability to localize and characterize objects hidden behind walls is highly desirable and has the potential to save countless lives. Multiple technologies are applicable for through-the wall surveillance; however, Ultra Wideband (UWB) technology provides a fine tradeoff between image resolution and penetration and is well suited for localization and characterization of objects behind a wall. The UWB radar system involves development of a comprehensive and portable solution for Through-Wall Vision.

Radar principle of operation has been used for the design and development of the system. An antenna system comprising of Vivaldi array and Wilkinson power divider transmits electromagnetic waves in the range of 3-6 GHz in a certain direction, which strikes the wall and penetrates it, after hitting the target reflects back and is received back after some time at the antenna system. Information about the target is then extracted from the received signal. Image is extracted after applying some image processing techniques on the data received from the vector network analyzer.

DEDICATED TO OUR BELOVED FAMILIES

ACKNOWLEDGEMENTS

We would like to thank our Project Supervisor Dr. Naveed Iqbal Rao who supervised the project. His support and guidance has been a valuable asset for our project.

We truly indebted to our co supervisor Asst. Prof. Zeeshan Zahid and Lab. Engr. Sara Viqar for taking intense academic interest in this project as well as providing valuable suggestions.

We would like to extend our gratitude to the staff of Image Processing Center, Microwave and RF Research Lab at Military College of Signals for providing us an environment to work to the best of our abilities.

TABLE OF CONTENTS

LIST OF TABLES

LIST OF FIGURES

LIST OF SYMBOLS/ABBREVIATIONS

2D	*Two Dimensional*
3D	*Three Dimensional*
3G	*Third Generation (Mobile Telecommunication)*
ADS	*Advanced Design System*
CW	*Clockwise*
CCW	*Counter Clockwise*
CWSA	*Constant Width Taper Slot*
DAC	*Digital-to-Analogue Converter*
dB	*Decibels*
E or H-plane	*Electrical or Magnetic plane*
FCC	*Federal Communications Commission*
FPGA	*Field-programmable Gate Array*
GSM	*Global System for Mobiles*
HFSS	*High frequency structure simulator*
HPBW	*Half Power Beam Width*
IF	*Intermediate Frequency*
LTSA	*Linear Tapered Slot Line*
LPDA	*Logarithmic Periodic Dipole Antenna*
LAN	*Local Area Network*
MMSE	*Minimum Mean Square Error*
PC	*Personal Computer*
RAM	*Radiation Absorbent Material*
RIMMS	*Research Institute of Microwave and Millimeter Wave Studies*
RF	*Radio Frequency*
S_{11}	*Reflection parameter from port 1 to port 1*
S_{21}	*Reflection parameter from port 2 to port 1*
SEECS	*School of Electrical Engineering and Computer Science*
TEM	*Transverse ElectroMagnetic*

TWMI	*Through the wall microwave imaging*
TSA	*Tapered Slot Antenna*
USRP	*Universal Software Radio Peripheral*
UWB	*Ultra-wide Band*
VNA	*Vector Network Analyzer*
WPD	*Wilkinson Power Divider*

Chapter: 1

INTRODUCTION

1.1 Problem Statement

The ability to see through walls is of high interest to many organizations including military, law enforcement and rescue agencies. We are able to see things around us based on the laws of reflection of light. However, these laws limit us from seeing through opaque objects such as walls, doors and other such obstacles. It has always been a desire to see through the walls as the information about the objects present behind a wall is of critical importance for search and rescue operations. Hence there is a need for an imaging device that can give real-time information about the precise location of different objects across opaque walls and obstacles. The surveillance device used for this purpose has to be portable, quick to deploy, easy to handle and covert in nature.

1.2 Objectives

Our research was centered on the design and development of a real time through-wall imaging prototype system, having utilization in the fields of defense and rescue operations. The project goals are as following:

i. Designing and development of a dedicated ultra-wideband antenna for Microwave imaging applications.

ii. Designing and development of an efficient Power Divider network for feeding the antenna system.

iii. Designing and development of a 2D antenna movement mechanism.

iv. Interfacing of the Vector Network Analyzer with the computer for data extraction and image construction.

1.3 Applications

Through the wall imaging is a capability that has very broad and important applications. This ability can be the difference between success and failure, for individuals and groups who operate and work in military, law enforcement, healthcare and emergency rescue.

i. **Military.** In most scenarios, military operatives enter potentially hostile situations without the knowledge of what is 'beyond the wall'. [2] The system will offer a comprehensive solution for 'Through-Wall Vision' within enclosed structures.

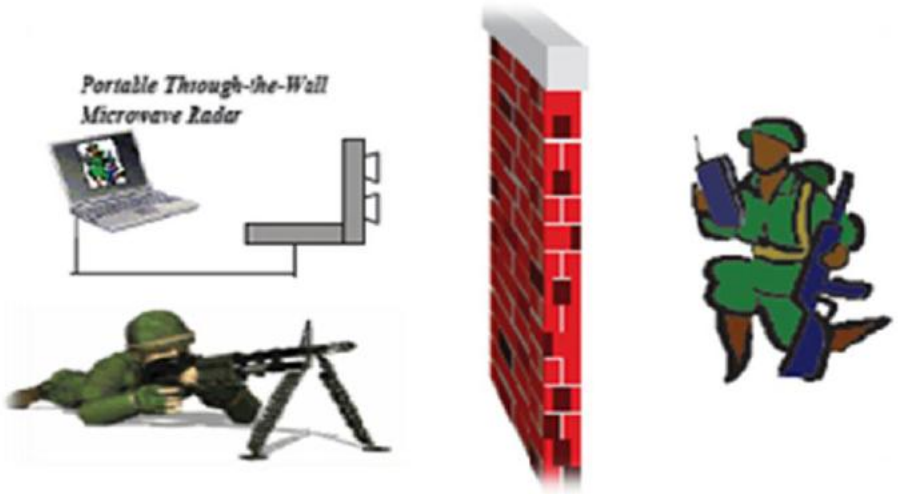

Figure 1-1 - Defense Application

ii. **Law Enforcement.** Law Enforcement personnel place their lives at risk on a daily basis in the pursuit of criminal justice objectives in urban environments. As shown in Figure 1-1, the system will allow effective preparation prior to an operation, thereby, increasing the chances of mission's success while reducing the risk to the operators participating in the mission as well as those on the other side of the wall. [2]

Figure 1-2 - Law Enforcing Agencies in Hostage Rescue Situation [3]

iii. **Healthcare.** The system will provide a less-intrusive imaging solution in the field of medicine using safer doses of radiation. The power level transmitted is minimal to avoid any danger to humans and other living beings. This technique could be used instead of traditional X-rays which have higher levels of radiation so have a limited usage per person. [4]

iv. **Emergency Rescue**. Investigation of the objects behind an opaque wall is a very promising field for a rescue and security applications nowadays. [5] As shown in Figure 1-2, using through-the-wall imaging technology, firefighters could distinguish between empty rooms and resident rooms and, hence, can save lives more effectively. Similarly help can be provided to those who are buried under the debris in case of earth quake or a disaster. [6]

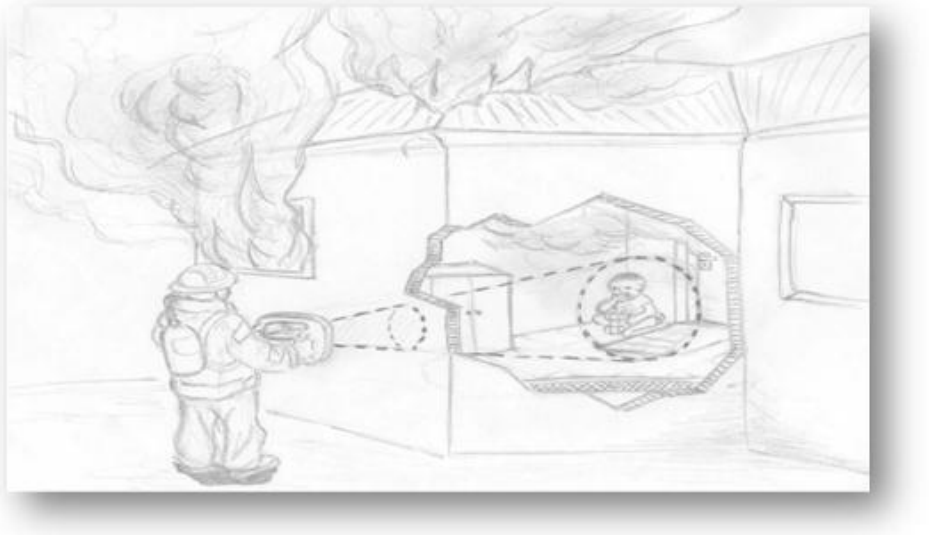

Figure 1-3 - Fireman Scanning the Room on Fire [3]

1.4 Methodology

The project involves development of a comprehensive solution for Through-Wall Vision. The project includes development of a broadband smart antenna system, which acts a sensor in simple terms and allows through-wall detection and localization of humans and metallic objects. It also includes a portable framework for antenna steering mechanism in order to facilitate efficient target detection and localization across the walls. The system is connected to a computer, where all the acquired data is received and processed. Several signal and image processing techniques are then applied to display reconstructed image of across the wall objects.

1.5 Proposed Model

The proposed model primarily consists of broadband smart antenna system which comprises of Vivaldi antenna arrays, WPD network and the phase shifting module for controlling the relative phases in an antenna array. The UWB radar transmits a signal and then looks for the reflected copy of it after a certain time-delay. This antenna is connected to Vector Network Analyzer. The RF waveform received is periodically sampled by the VNA to obtain digital data. This digital data is then sent to a computer via an interface, where signal and image processing techniques are applied for

reconstructing the through-wall images. The project block diagram is shown in Figure 1-4 below.

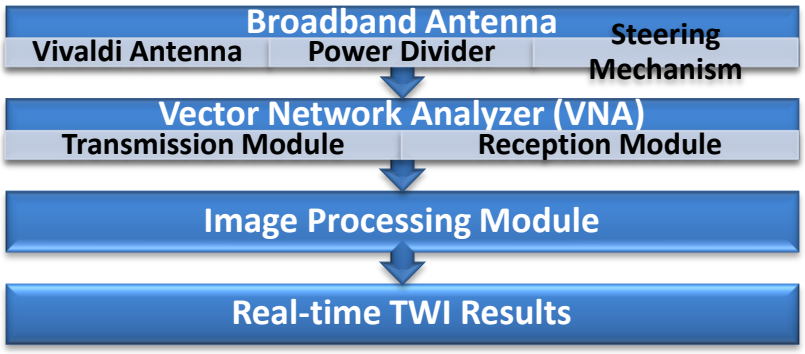

Figure 1-4 - System Block Diagram

The project has been carried out in five modules as shown in Figure 1-5.

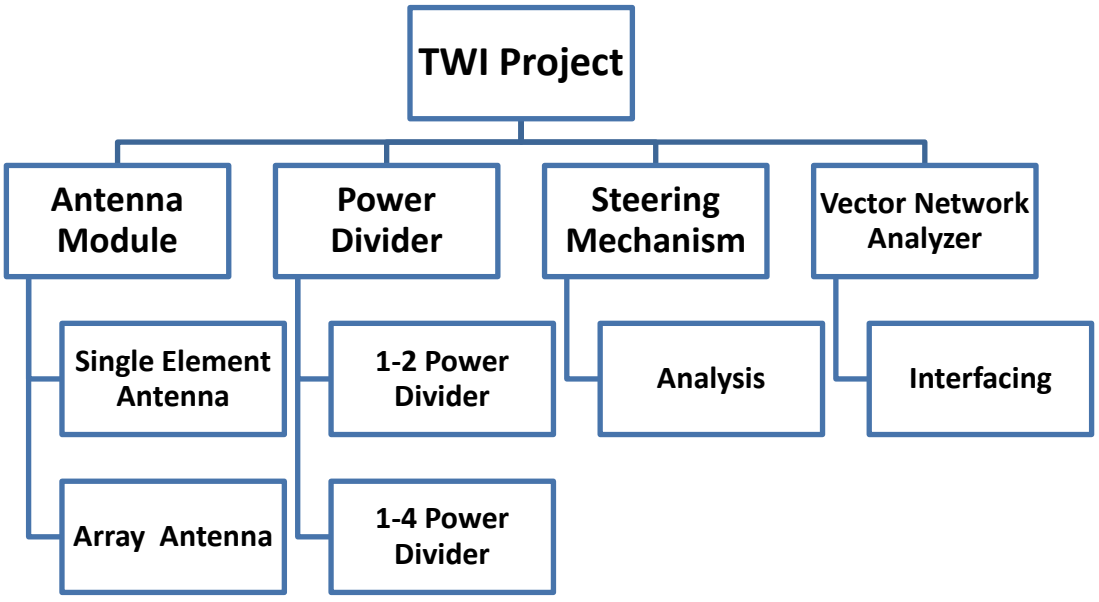

Figure 1-5 - TWI System Modules

Chapter: 2

ANTENNA SELECTION AND DEVELOPMENT

2.1 Introduction

A wideband antenna is needed to attain a narrow transmitting pulse in time domain. Narrow pulse provides better resolution and measurement sensitivity against frequency dependent material properties can be minimized. Microwave applications, electromagnetic compatibility testing and standard measurements require the antennas to have high bandwidth along with high gains.

2.2 Antenna Requirements

From the RADAR signal processing view point, designing of any imaging system with satisfactory performance, such as ability to detect and distinguish moving and stationary objects, their dimensions, speed and locations, an antenna must satisfy some of the requirements including; optimum performance in desired frequency range, it should not have large electrical size either to be spatially big or to have a wide bandwidth, or, even better, to possess both features. These features are responsible for spatial, or range, resolution, both azimuth and elevation, It should have a reasonable gain, It should have a directional radiation pattern so that most of the radiated power is concentrated in a narrow beam and we do not get unwanted reflections for other objects, It should be physically small, low-profile and low-cost. All these features are important to create low-cost, convenient TWI system, it should be easy to mount, easy to match, have good transmission and radiation performance.

Before designing an antenna for TWI, we need to select appropriate frequency range. We want our signal to have enough penetration through wall and resolution is required to get precise location of the objects present behind the wall. It is known that at lower frequencies we get more penetration but at the same less resolution. Similarly at higher frequencies we can have more resolution (due to smaller wavelengths) but less penetration [15]. So a tradeoff is required. An antenna for frequency range 3 to 6 GHz is to be designed. High frequency structure simulator (HFSSv13) is used to design the

antenna as it has been observed that its simulated results closely resemble manufactured results.

2.3 Selection of Antenna

For a light and portable Through-the-Wall Imaging (TWI) solution, the transmitting and receiving antennas must not be heavy and bulky. Furthermore, the antenna must transmit UWB pulses with minimal distortion and high efficiency. Significant image distortion arises because of the faulty antenna radiation pattern, hence it needs to be accounted. [9] Multiple antennas were evaluated on the basis of their key parameters, namely Impedance Bandwidth, Radiation Efficiency, Physical Size, Weight and Directivity, to cater for all these antenna design parameters. The results of the evaluation process are as shown in Table 2-1.

Table 2-1 - Antenna Comparison [10]

Antenna	Impedance Bandwidth	Radiation Efficiency	Physical Size	Weight	Directivity
Dipole	Narrow	High	Small	Light	Low
Loop	Narrow	High	Small	Light	Low
Bow Tie	Medium	High	Medium	Light	Low
Diamond	Medium	High	Medium	Heavy	Low
Vivaldi	Wide	High	Medium	Light	High
LPDA	Wide	Medium	Large	Medium	Low
Spiral	Wide	Medium	Large	Medium	Medium
Bicone	Wide	High	Large	Light	Low
TEM	Wide	High	Large	Heavy	High

For TWI application, Vivaldi antenna because of its simple structure, less weight, small lateral dimensions, wide bandwidth, high efficiency and high gain characteristics has been selected.

2.4 Vivaldi Antenna

Vivaldi antenna was proposed by Gibson in 1978 and since then it has been employed in various research and developmental areas. [11]. Usage of printed circuit technology has made these antennas simple and economical. The antenna finds its use in fields such as microwave imaging and in ground penetrating radar systems due to its ultra-wideband designs.

2.4.1 Antenna Taper

Tapered-Slot Antennas (TSA) are used in various taper slot profiles. Figure 2-1 shows various designs in which the antenna can be used, these planar design differs from each other on the basis of slot structure. There are two features which are common in all these designs; balanced slot line is used as antenna feed and the radiating slot acts as the antenna ground plane. [12] A TSA with an exponential flare slot profile makes a Vivaldi antenna.

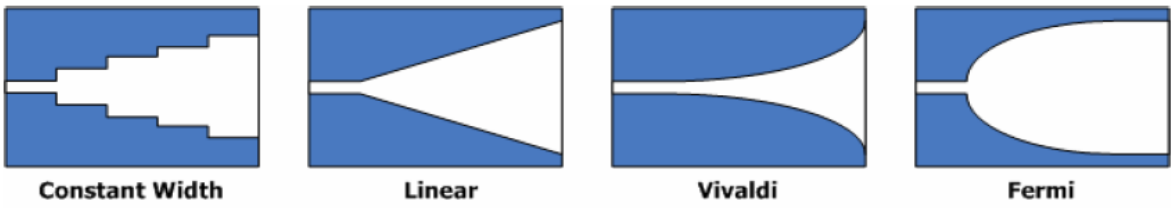

Figure 2-1 - Various Tapered Slot Antenna [13]

2.4.2 Principle of Operation of Vivaldi Antenna

Vivaldi antenna is a travelling-wave antenna of the "surface-type", containing an exponentially widening flare. Sources and diodes are connected at the thinner end of the slot for best matching and coupling. Waves are tightly bound in the region where the separation between the conductors is less in comparison with the wavelength of free-space, this bonding gradually becomes weaker as the separation increases. [11]

Tapered-slot antennas radiate at the wider end of the slot in the end-fire direction in preference to other directions due to traveling waves propagating along the antenna structure as the phase velocity (v_p) is less than the velocity of light in free space i.e.

$v_p < c$. Also, by varying the antenna parameters such as dielectric constant, thickness and taper design the phase velocity and the guide wavelength can be varied. [14] The antenna has symmetric radiation pattern.

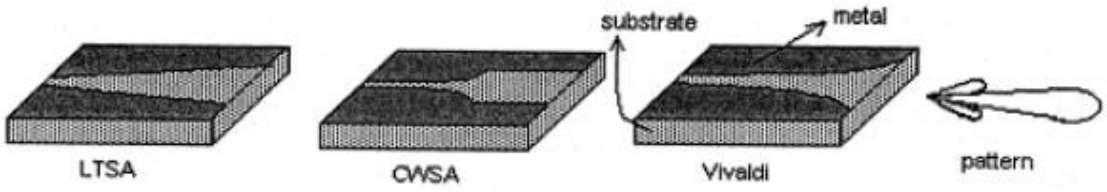

Figure 2-2 – Tapered Slot Antenna Radiation Pattern [15]

Theoretically, the antenna has infinite bandwidth and because of this reason it is also termed as frequency independent because different parts of the antenna radiate at different frequencies. Vivaldi Antenna has a very high bandwidth due to the variation in wavelength as different sections of the antenna radiate. [12]

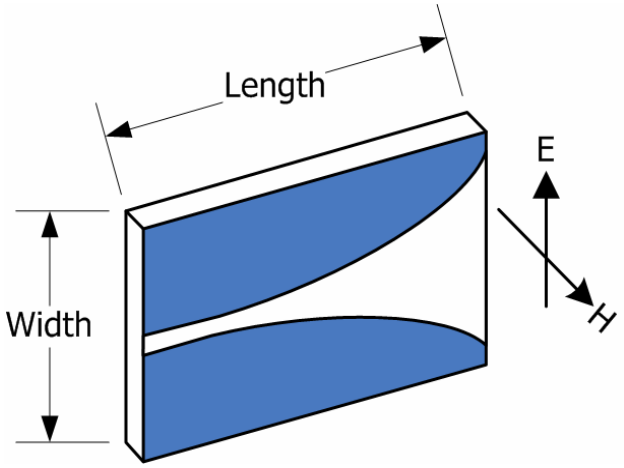

Figure 2-3 - Taper Structure of Vivaldi Antenna [13]

2.5 Vivaldi Single Element Design

The final single element design is as shown in Figure 2-4. The antenna has been designed on FR4 Epoxy substrate with a relative permittivity (ε_r) of 4.4 and a thickness of 1.6mm. The operational range of the antenna is 3-6 GHz and a port impedance of 50Ω. The antenna was designed and optimized using Ansoft HFSS software.

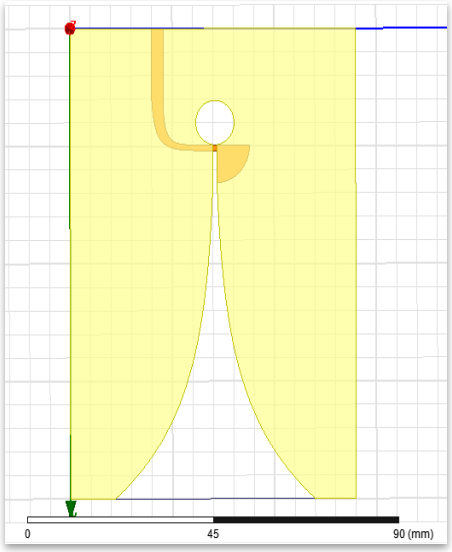

Figure 2-4 - Design of Single Element of Vivaldi Antenna

2.6 Parameter study: An overview

Various design parameters of the strip-line-fed Vivaldi array antennas were analyzed to enhance the wideband performance in a systematic procedure.

The following were some of the parameters taken into consideration in the parameter study:

- Diameter of the slot-line cavity and the strip-line stub
- Input strip-line and slot-line width
- Taper profile
- Aperture height

The antenna performance is affected by changing these parameters. Antenna resistance can be increased which results in a decrease in minimum operating frequency, through proper change in design parameters. The higher end of the bandwidth is set by the onset of grating lobes and hence only way to improve the bandwidth is by decreasing the lower cutoff. Effect on the antenna impedance was observed by varying these parameters one at a time. Important relationships were identified between the design of the antenna and the performance of each of the elements. The above parameters were studied for different combinations of substrate thickness and strip-line & slot-line characteristic impedances.

Design possibility that showed the largest bandwidth, gain and directivity was selected for the actual design.

2.6.1 Introduction

The strip-line-fed Vivaldi antenna comprises:

- The strip-line-to-slot-line transition.
- The strip-line open circuit stub and slot-line short circuit cavity.
- The radiating tapered slot.

Figure 3-1 is a snapshot of the Vivaldi element as modeled in HFSS. The outside layers, viz., the top and the bottom layers (in red) are identical tapered slot-lines which also act as ground planes for this antenna. The middle layer is the strip-line plane (in green) that is used as the connection to the signal input or any test equipment.

These three layers together form the Vivaldi antenna. The input signal is fed to the strip-line input and is then magnetically coupled to the slot-line on either sides of the board. The input impedance of the antenna is dictated by the strip-line while the operating bandwidth of the antenna is governed by the strip-line-to-slot-line transition.

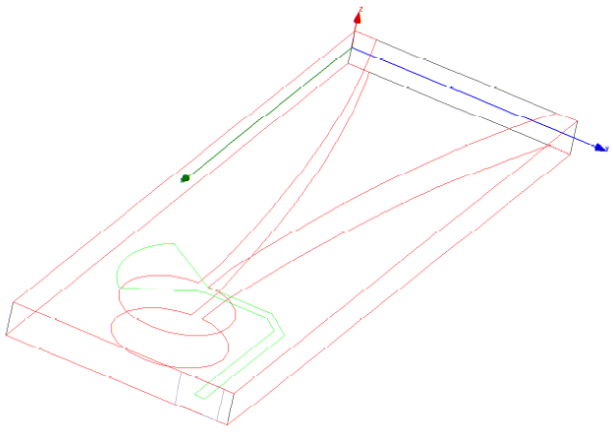

Figure 2-5 - Single Vivaldi Element

It was shown by Yngvesson [9] and Gibson [5] that single-element Vivaldi antennas work best when they are over a wavelength long and when the height of the antenna aperture is greater than one-half wavelength. In the case of arrays, on the other hand,

good performance is obtained from antennas that are less than a wavelength long and when the element heights are much less than a wavelength. Typically, a single element in an array is unmatched almost throughout the bandwidth of interest. However, by proper array design, mutual coupling between the elements can be constructively used and very wideband behavior could be accomplished.

2.6.2 Substrate material

Dielectric substrate are the most important component in antenna design and simulation. Some characteristics of the dielectric substrate are:

- The dielectric constant.
- The dielectric loss tangent and the dielectric loss.
- The thickness of the copper surface.
- The thermal expansion and conductivity.
- Cost and manufacturability.

A wide variety of substrates having different properties can be employed in the design and development process of antennas. Using thick substrates with low dielectric constant results in large bandwidth. But this also results in an appreciable decline in gain. Therefore, there must be a design trade-off between antenna gain, size and good antenna performance.

2.6.3 Feed mechanism

The antenna bandwidth is defined by the feeding mechanism of the antenna. In this section, the design of a strip-line to slot-line transition as a feed mechanism is described. This design has been implemented based on the parametric study performed by Schubert and Shin [25], which basically makes use of the strip-line slot-line feed mechanism. The micro-strip to slot-line transition has lots of advantages over other mechanisms. This transition can be easily fabricated by normal photo-etching processes. Also, two-sided circuit boards are possible with the micro-strip on one side and the slot-line on the other.

2.6.3.1 Strip-line to slot-line transition

The micro-strip to slot-line transition (Figure 3.2) basically consists of,

- Strip-line, used as a connection to the transmitter/receiver circuitry.
- Slot-line, which is flared outwards from the feed.

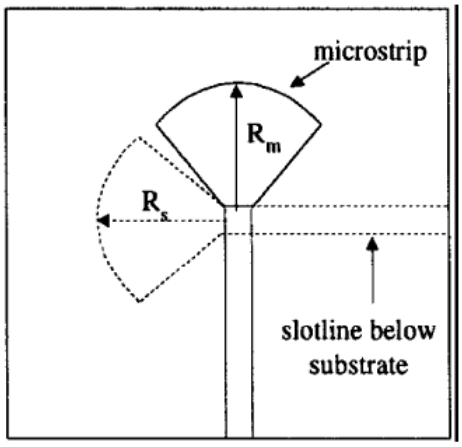

Figure 2-6 – Micro-strip to Slot-line Transition

The radial stub used here eliminates the problem of overlapping of the stubs and also provide better bandwidth than the other two. [20]

The stubs extend a quarter-wavelength further from the crossing point. Due to this quarter-wavelength transformation at the overlap, the strip-line open circuit stub appears as a short circuit while the slot-line short circuit appears as an open circuit. Designing a good quarter-wavelength stub is crucial to obtain a fairly wideband transition.

$$Z_0 = \frac{\eta_0}{2\pi\sqrt{\varepsilon_r}} ln\left\{1 + 0.5\frac{8b}{\pi w'}\left[\frac{8b}{\pi w'} + \sqrt{\left(\frac{8b}{\pi w'}\right)^2 + 6.27}\right]\right\} \quad \text{... (1)}$$

$$2h = b \quad \text{… (2)}$$

$$w' = w + \frac{\Delta w}{t}t \quad \text{… (3)}$$

$$\frac{\Delta w}{t} = \frac{\ln(\frac{5b}{t})}{3.2} \quad \text{… (4)}$$

Where:

‘b’: thickness of strip-line substrate

'w': strip-line width

't': thickness of conductor

Z_0: Characteristic impedance of the strip-line

The use of the radial/circular stubs have been shown to achieve a significantly better bandwidth than the uniform stubs. Moreover, designing non-uniform stubs is easier with modern etching processes.

2.6.4 Slot-line design

The slot-line plane of the antenna consists of the circular slot-line cavity, the uniform slot-line input and the tapered radiating slot, as shown in Figure 3-4.

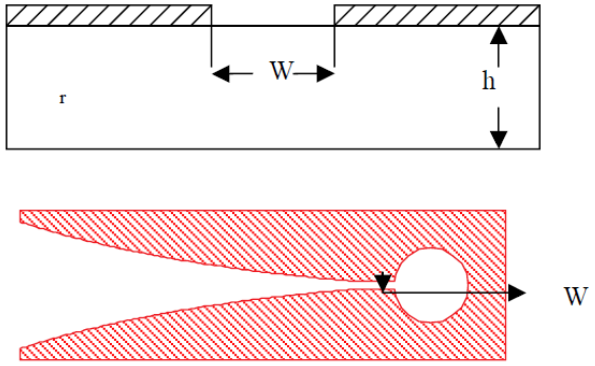

Figure 2-7 – Slot-line Design

The slot-line width at the transition region was chosen to be 1 mm. As reported by Schubert, this transition setup worked well in a frequency range between 1 GHz and 6 GHz [25]. The slot-line wavelength and the characteristic impedance were calculated using equation () and (). The formulae specified are empirical and not in any case exact. The center frequency of 4 GHz is chosen for all the calculations with the substrate parameters being the same.

$$2.22 \leq \epsilon_r \leq 9.8 \qquad \ldots (5)$$

$$0.0015 \leq \frac{W}{\lambda_0} \leq 1 \qquad \ldots (6)$$

$$0.006 \leq \frac{h}{\lambda_0} \leq 0.06 \quad \ldots (7)$$

$$\frac{\lambda_s}{\lambda_0} = 1.045 - 0.365 ln\varepsilon_r + \frac{6.3\left(\frac{W}{h}\right)\varepsilon_r{}^{0.945}}{238+100\frac{W}{h}} - \left[0.148 - \frac{8.81(\varepsilon_r+0.95)}{100\varepsilon_r}\right] \times ln\left(\frac{h}{\lambda_0}\right) \ldots (8)$$

$$Z_{os} = 60 + 3.69\sin\left[\frac{(\varepsilon_r-2.22)\pi}{2.36}\right] + 133.5\ln(10\varepsilon_r)\sqrt{\frac{W}{\lambda_0}} + 2.81[1 - 0.11\varepsilon_r(4.48 + ln\varepsilon_r)]\left(\frac{W}{h}\right)\ln\left(\frac{100h}{\lambda_0}\right) +$$

$$131.1[1.028 - ln\varepsilon_r]\sqrt{\frac{\mathrm{h}}{\lambda_0}} + 12.48(1 + 0.18ln\varepsilon_r)\frac{\left(\frac{W}{h}\right)}{\sqrt{\varepsilon_r-2.06+0.85\left(\frac{W}{h}\right)^2}} \quad \ldots (9)$$

The lowest frequency of operation of the antenna is decreased by increasing the size of cavity (when in an array) which results in an increase in bandwidth. To test the frequency response of the transition, two transitions were cascaded together on a FR4 Epoxy substrate. This setup was then modeled in Ansoft HFSS.

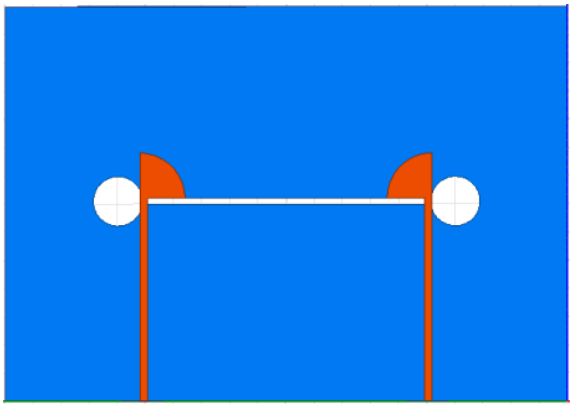

Figure 2-8 – Dual Slot-line Transition

The S11 result in Figure 3-6 shows that this transition is wideband with the S11 less than -10 dB throughout the required bandwidth of 1.6-7.8 GHz

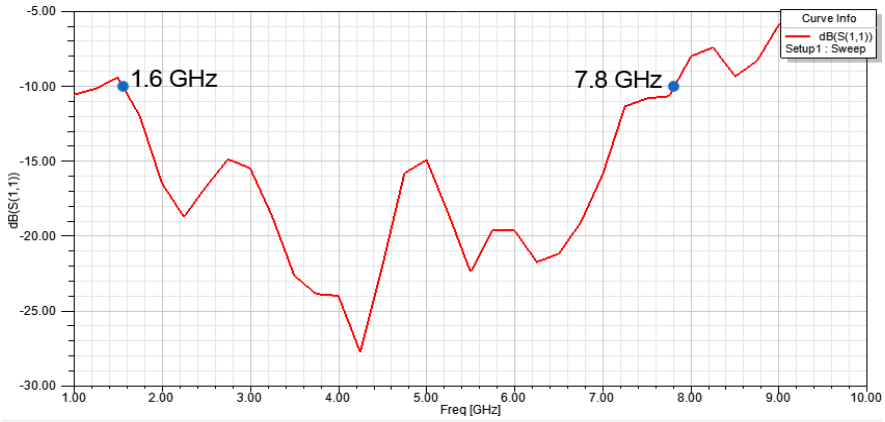

Figure 2-9 – Return Loss Plot of Dual Slot-line Transition

2.6.5 Taper design

As discussed in the previous chapter, the TSA with an exponential taper is referred to as the Vivaldi antenna. Numerous exponentials have been used in the literature [3], [18], [20], [25]. Schubert, in his design, has used the following exponential relations to design the taper. With reference to Figure 3-7, R is the taper opening rate and the points P1 (z1, y1) and P2 (z2, y2) are the start and end points of the taper profile respectively. A closer look will reveal that P1 is actually the point where the slot-line. The difference z2 – z1 is the flare length L, as shown in the picture below. It is worth mentioning that when R becomes zero, the slope of the taper becomes constant resulting in a linearly tapered profile.

$$y = c_1 e^{Rx} + c_2 \qquad \ldots (10)$$

$$c_1 = \frac{y_2 - y_1}{e^{Rx2} - e^{Rx1}} \qquad \ldots (11)$$

$$c_2 = \frac{y_1 e^{Rx2} - y_2 e^{Rx1}}{e^{Rx2} - e^{Rx1}} \qquad \ldots (12)$$

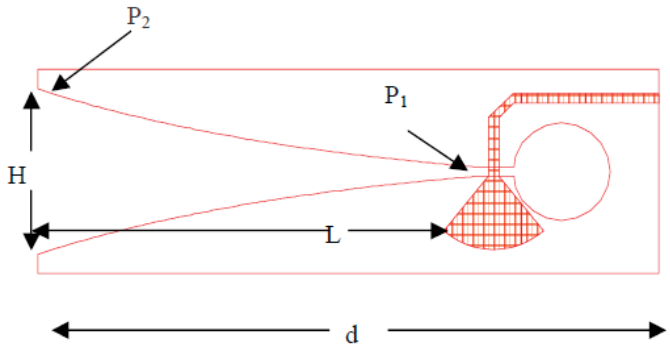

Figure 2-10 – Taper Design of Vivaldi Antenna

It was observed that as the length of the taper is increased, for the same aperture height, the flare angle is reduced correspondingly. It was reported [25] that for small flare angles, the lowest operating frequency of the array reduces and subsequently the bandwidth increases. Similar study was also done for the opening rate R of the exponential flare. For larger opening rates, the flare angle becomes small at the origin and the lowest frequency of operation reduces as before. Further increase produces significant improvement in the SWR at the higher operating frequencies.

2.7 Simulation Results

The reflection co-efficient plot of the individual Vivaldi antenna is displayed in Figure 2-7. S_{11} parameter also known as return loss, is the ratio between the reflected power and the transmitted power. This value is required to be as minimal as possible so that the device can radiate the maximum power. Greater the value of S_{11}, lower is the efficiency of the device and vice versa. In microwave devices, -10 dB is used as general criteria for the efficiency of the device. As can be seen, the device has matched performance in the range of 1 to 6 GHz.

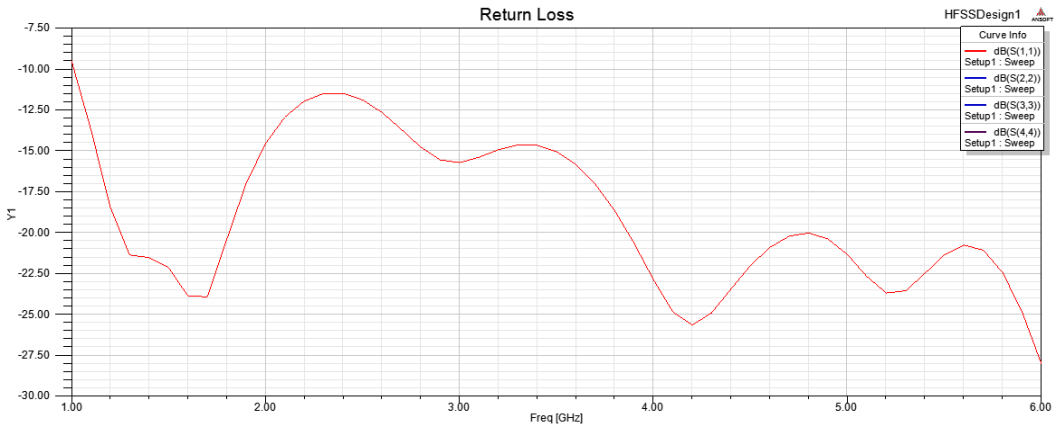

Figure 2-11 - S_{11} Plot of Single Element Antenna

In section 2.3.1, different empirical formulae were discussed related to the performance of the Vivaldi antenna. According to the empirical formula, the directivity of the antenna is 9.64 dB. The simulated directivity and gain patterns are as shown in Figure 2-8 and 2-9 respectively. As can be seen, the antenna provides a peak directivity of 9.59dB and a peak gain of 9.21 dB.

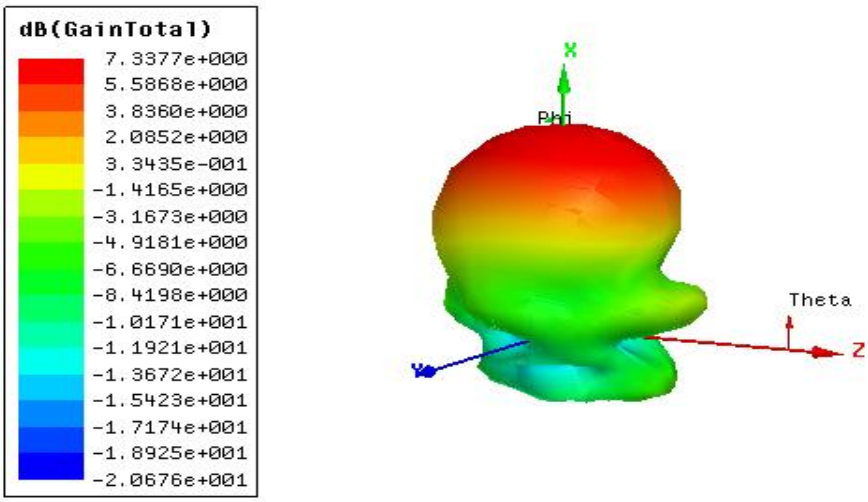

Figure 2-12 - 3D Directivity Plot of Single Element Antenna

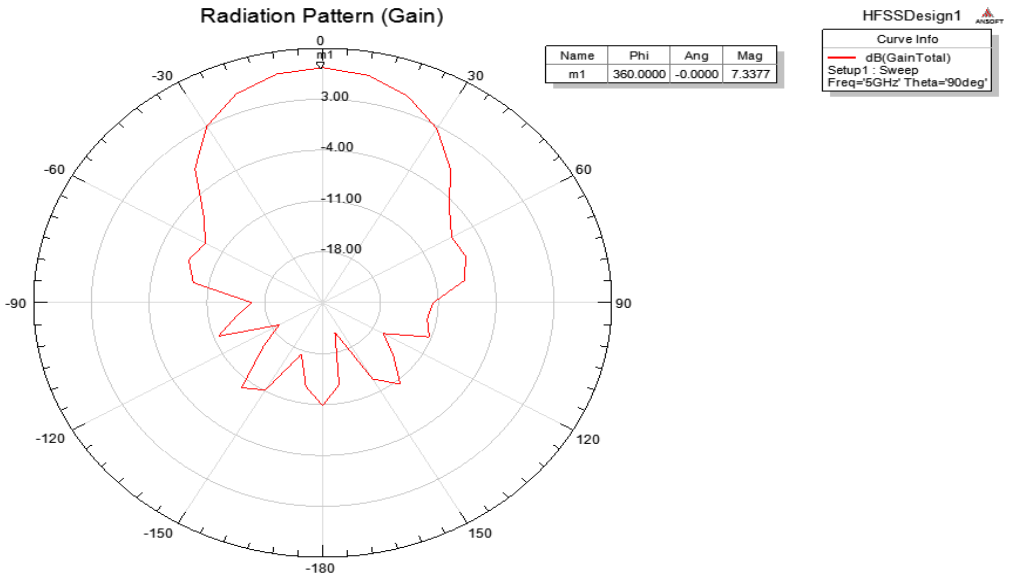

Figure 2-13 - 2D Gain Plot of Single Element Antenna

2.8 Array design

2.8.1 Introduction

Single element configuration provides very low gain which hampers the through wall imaging process. As explained earlier, an array configuration would help in building smaller antenna elements rather than realizing large single antennas. Radiation pattern of an array is determined by the type of the individual element used, their orientations, their positions in space, and the amplitude and phase of the currents feeding those [30]. The basic array pattern consists of two parts, the pattern of one of the elements by itself which is aptly called the element pattern and the pattern of the array with the actual elements replaced by isotropic sources, referred to as the array factor. The total pattern of the array is then the product of the element pattern and the array factor.

2.8.2 Array factor

The basic configuration of an array antenna is the linear array. As the name suggests, it is an arrangement of the antenna elements in a single straight line with the appropriate feed network. To determine the array factor, the elements are assumed to be point sources that radiate equally in all directions, commonly known as isotropic radiators, but retaining their respective locations. The distance of separation between the elements is very

crucial in the proper design of the array. This distance dictates the phase difference between the elements and is inherent to the array.

It is really intuitive to arrive at the array factor for a small linear array, given its setup and input feed characteristics by what is called the inspection method. Consider a linear array of two elements and no additional phase shifting given on the inputs. At the far-field of the antennas, the waves arriving from the elements on an axis perpendicular to the line joining the two sources, add in phase and hence we would see a field maximum in that region. On the other hand, along the axis of the array, the waves cancel each other at the far-field due to the phase difference created by the separation between the two sources.

2.8.3 Mutual Coupling

The inspection method, though intuitive cannot be used for more complex arrays with more number of elements and complex phase differences and distance of separation. Moreover, all these derivations have been based on the assumption that all the elements are isolated from each other and from external sources. However, in practice, this is rarely the case. Each element interacts with all the other elements in the array creating what is known as the mutual coupling which causes changes in the current magnitude, phase, and distribution on each element. The end result is that the total array pattern is different from the no-coupling case. Mutual coupling not only depends on the proximity of the elements, but also on the frequency and scan direction. Also, it was found that mutual coupling decreases as the spacing between elements increases and that the coupling strength is predicted by the far field pattern of each of the elements.

This is referred to as the driving-point impedance. It is evident that input impedance of each element depends on the mutual impedances with the other elements in the array and the terminal currents.

2.9 Vivaldi Array

Single element Vivaldi antenna provides a low gain of 7.34 dB, which is not sufficient for through wall imaging. Vivaldi array antenna has been designed in a 1x2 linear

architecture comprising of two single Vivaldi elements as shown in Figure 2-10, to increase gain and directivity. To avoid mutual coupling of individual elements in the array and to achieve higher directivity, an inter element spacing of 0.8λ has been introduced between the individual Vivaldi elements.

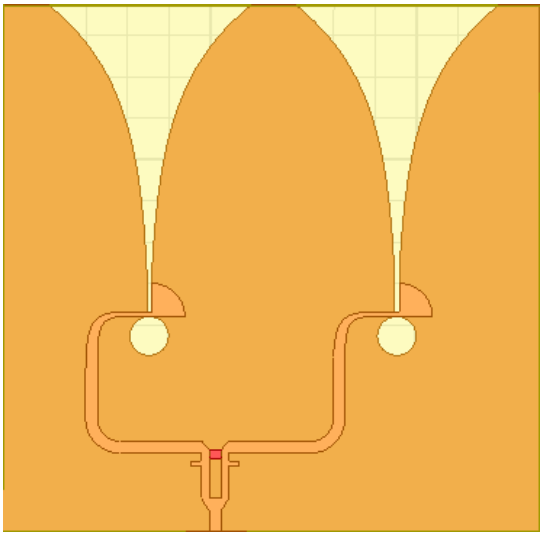

Figure 2-14 - Vivaldi Array Antenna Design

Two antenna elements placed near each other will have an exchange of radiated energy between them resulting in an undesirable effect called mutual coupling. As per Figure 4-1, energy radiated from antenna n (0), besides being radiated into space (1) will be re-scattered, coupled to (2) and will enter antenna m (4). At the same time with antenna m also radiating (3), part of its energy will also be re-scattered and coupled to antenna n (5). [21] This coupling of energy is actually a vector addition of the incident and reflected waves of each radiating element, influencing the input impedance looking in at the terminals of each radiating element, referred to as mutual impedance variation.

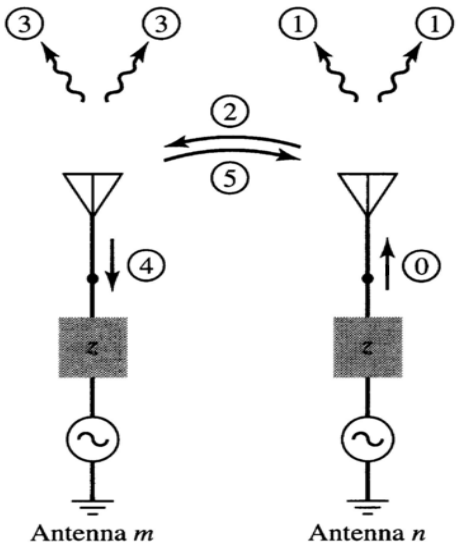

Figure 2-15 - Mutual Coupling in Multiple Antenna Systems [21]

Mutual coupling can seriously complicate the design and analysis of antenna systems and in practical cases is difficult to predict and analyze.

2.10 Integrated Antenna Design

As the antenna and the power divider were designed and simulated separately, therefore, in order to see the mutual coupling effect of the complete design, the two modules were combined to form an integrated setup. The integrated setup on FR4 epoxy substrate is as shown in Figure 4-2 to get a compact and more effective design.

In order to facilitate beam steering and provide additional gain, a 4x2 architecture has been proposed and simulated in Ansoft HFSS. The design is as shown in Figure 4-3.

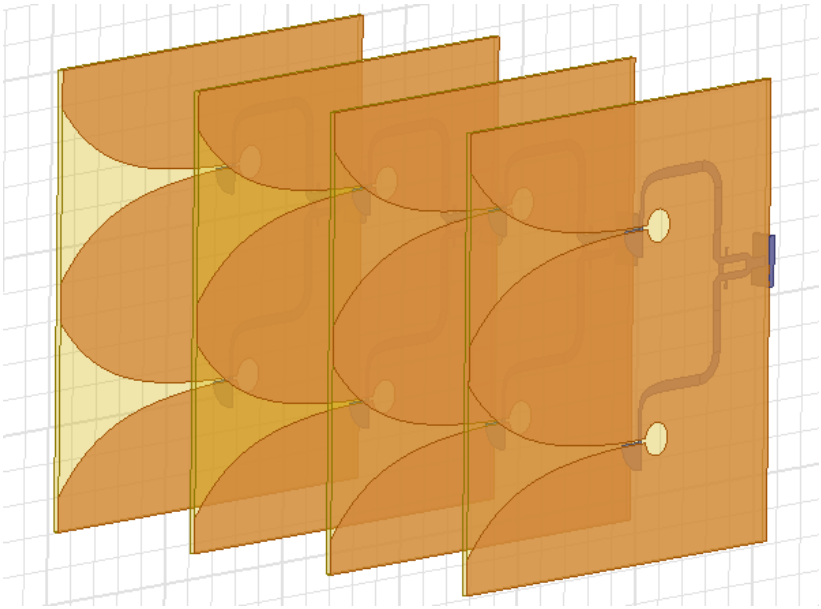

Figure 2-16 - Integrated Antenna Design (4x2)

As shown in Figure 2-11 and 2-12, the gain of the array comes out to be 12.83 dB.

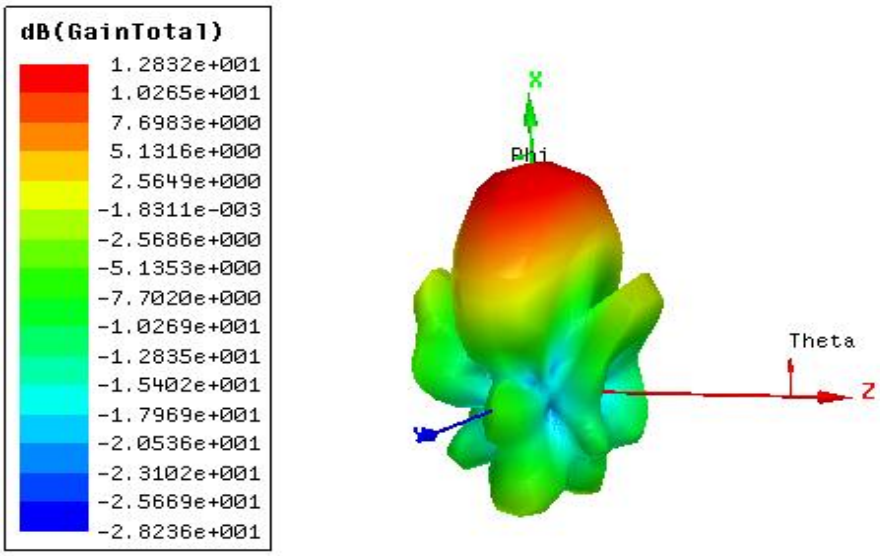

Figure 2-17 - 3D Directivity Plot of Array Antenna

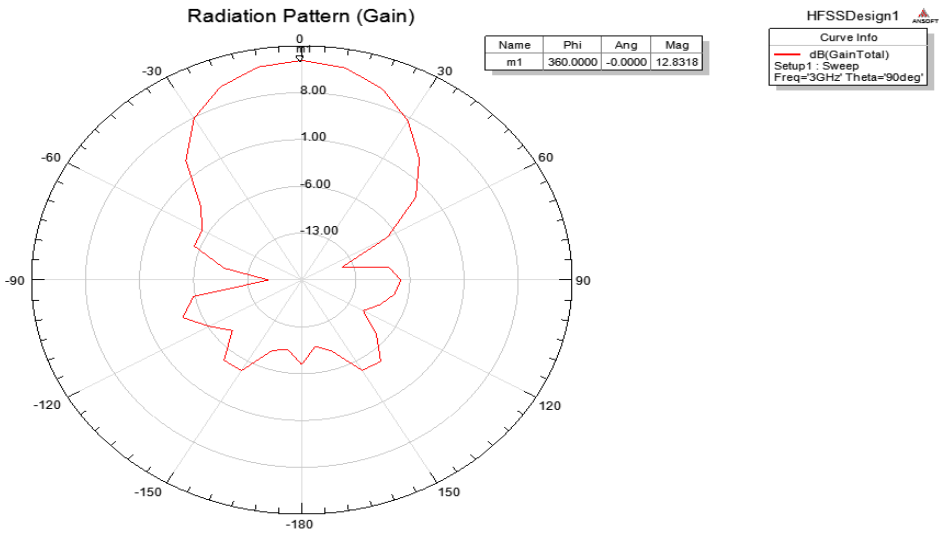

Figure 2-18 - 2D Gain Plot of Vivaldi Array Antenna

2.11 Summary

Keeping in view the goal and objectives of the project, a Vivaldi antenna was selected from multiple antennas as it qualified the selection criteria and requirements to be directive and ultra-wideband in nature. It was observed that the gain provided by a single element of Vivaldi is low, whereas high gain is an essential requirement in through the wall imaging applications. Hence an array of Vivaldi antenna elements has been constructed. The array of Vivaldi antenna gives met the gain, directivity and bandwidth requirements. Optimum performance is obtained by reducing the mutual coupling of individual elements by introducing an inter element spacing of 0.8λ between the individual Vivaldi elements and 0.667 λ between the two panels.

Chapter: 3

POWER DIVIDER SELECTION AND DEVELOPMENT

3.1 Introduction

Feed of the network is one of the most crucial issue of an antenna setup. Each port of the four-element linear Vivaldi antenna has to be fed with the same input power level and phase offset. The antenna array can be driven from a single source by using a 1:4 power divider. Power Dividers and combiners are passive devices which find their applications in a vast range of applications. So far, quite a lot of symmetric and asymmetric power divider structures have been proposed, including the T-Junction power divider, Wilkinson power divider and the Resistive divider. For the project, these power dividers were compared on the basis of their lossy nature, isolation between the output ports and the matching condition on the output ports. These comparison results are as shown in Table 3-1:

Table 3-1 - Power Divider Comparison [17]

Power Divider	Advantage	Disadvantage
T-Junction	• Simple	• Difficult to match • Highly inefficient isolation
Wilkinson	• Lossless • High isolation • Low VSWR	• Reflected power is dissipated through isolation resistor if not matched
Resistive Divider	• Easy to match	• High loss • No isolation

The Wilkinson power divider is the optimal choice as it fulfills the network condition of being lossless, reciprocal and matched.

3.2 Working

The matching of output ports makes the Wilkinson Power Divider (WPD) network lossless. Input power can be divided into two equal amplitude signals which have the

same phase. $\frac{\lambda}{4}$ Impedance transformers having a characteristic impedance of $\sqrt{2}Z_0$ and a lumped isolation resistor of $2Z_0$, has been used for a two way WPD. Fig 3-1 (a) shows the micro-strip design. The equal micro-strip transmission line circuit is displayed in Fig 3-1 (b).

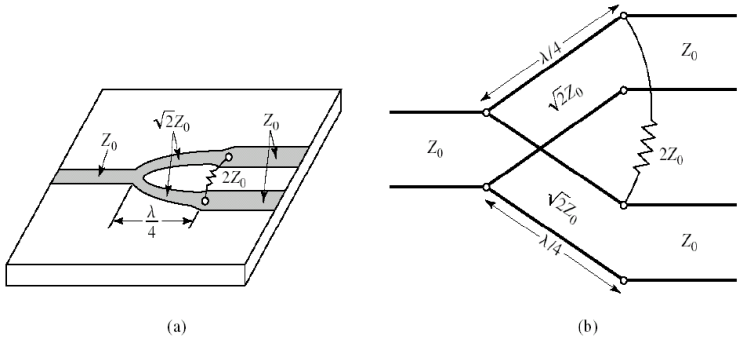

Figure 3-1 - Conventional 1-to-2 WPD [22]

When the signal enters the input port, it splits into two signals having equal amplitude and phase. Since both ends of the isolation resistor are at the same potential, no current flows through it. The resistor performs the major function of decoupling the output and input ports. The two output ports are isolated from each other as the signal at either port splits into two parts. Half of the signal goes clockwise through the resistor and the other half travels counterclockwise through the two quarter-wave transformers. The recombining signals at the other output port end up equal in amplitude but 180^O out of phase. The two signal voltages subtract to zero at the output port and the signal disappears. [22] This ensures that the output terminals are isolated from each other and, hence, do not interfere with each other.

3.3 S-Parameters

The 1-to-4 Wilkinson Power Divider is achieved by combing three 1-to-2 power dividers in cascade. The scattering parameters for the power divider are given as under

$$[S] = -\frac{1}{2}\begin{bmatrix} 0 & 1 & 1 & 1 & 1 \\ 1 & 0 & 0 & 0 & 0 \\ 1 & 0 & 0 & 0 & 0 \\ 1 & 0 & 0 & 0 & 0 \\ 1 & 0 & 0 & 0 & 0 \end{bmatrix} \quad \text{…….. (13)}$$

Inspection of the Scattering Matrix reveals the following:-

- Power divider is reciprocal ($S_{ij} = S_{ji}$)
- All ports are matched ($S_{ii} = 0$)
- Output terminals are isolated ($S_{ij} = 0$ for $i \neq 1$, $j \neq 1$ and $i \neq j$)
- Equal (6 dB) power division is achieved ($S_{21} = S_{31} = S_{41} = S_{51}$)
- Power divider is lossless ($\sum |S1j|^2 = 1$ for $j \neq 1$)

3.4 Wilkinson Power Divider

The Wilkinson Power Divider, as shown in Figure 3-2, is designed at 4 GHz for use in Through-the-Wall Imaging (TWI) applications. The proposed design is based upon the design given in [23], however, the design does not operate in wide band, therefore, the design is customized to get optimum results for 3-6 GHz frequency range by the addition of stubs.

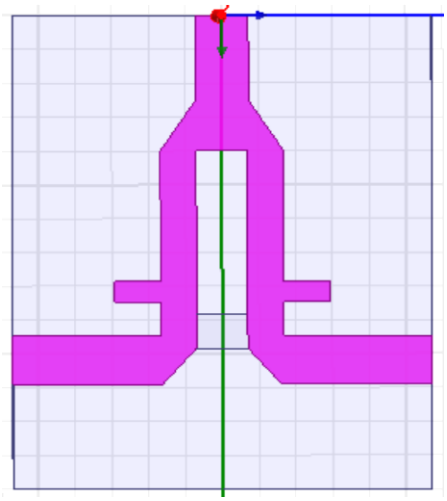

Figure 3-2 - 1-to-2 Wilkinson Power Divider

According to the experimental results, the 1-to-2 power divider has a size of 86 by 42 by 1.6 mm^3. FR4 Epoxy with 1.6mm thickness is used as the substrate instead of 0.508mm thick Rogers RT5880 substrate. FR4 is used as it is a cost effective and reliable material for multi-layered PCB-based applications and is also easily available. The design has been mathematically modeled and the results have been optimized using HFSS software. Three 1-to-2 WPD has been cascaded to form 1-to-4 power divider as shown in Figure 3-3.

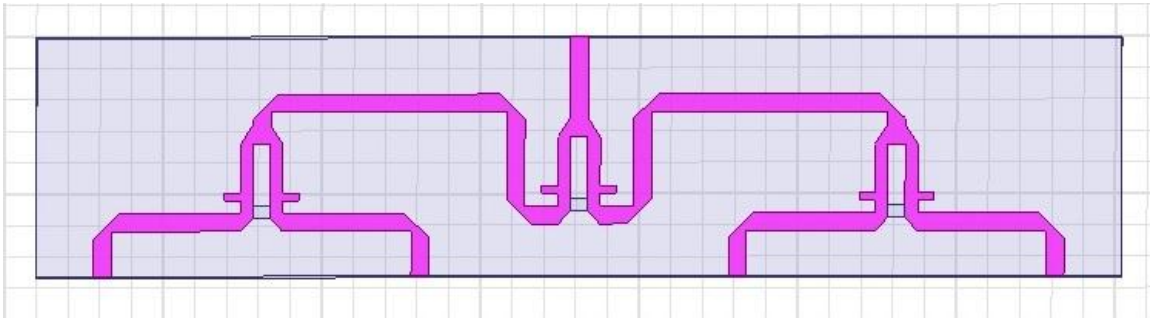

Figure 3-3 - Novel 1-to-4 Wilkinson Power Divider

3.5 Analysis

The Power Divider has been designed and optimized using the Ansoft HFSS software.

3.5.1 Reflection Co-efficient

The reflection coefficient at the input port, also known as impedance matching (S_{11}), achieved by the divider is as shown in the Figure 3-4. Impedance matching equal to -21.44dB for the input port at 4 GHz has been achieved. The Reflection Co-efficient remains below -10dB level from 2.42 GHz to 4.60 GHz, hence, the power divider is operational in this frequency range.

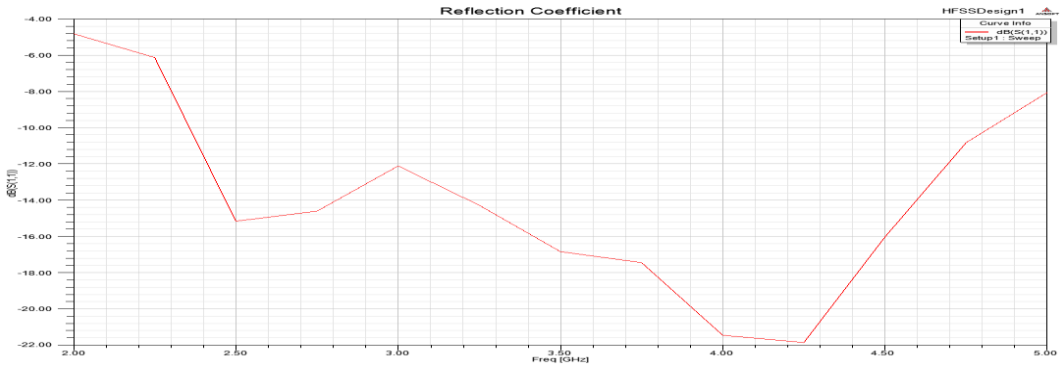

Figure 3-4 - Impedance Matching of 1-to-4 WPD

The design ensures that all ports are matched with characteristic impedance (Z_o) of 50Ω at all frequencies to minimize mismatch losses. The four output ports of the novel divider are also perfectly matched and their reflection coefficients (S_{22}, S_{33}, S_{44} and S_{55}) are plotted in Figure 3-5.

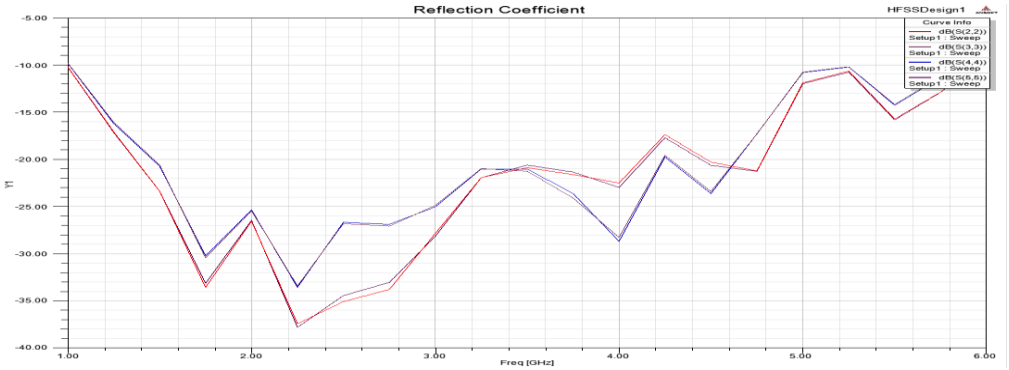

Figure 3-5 - Reflection Co-efficient of 1-to-4 WPD

3.5.2 Isolation Factor

Isolation Factor of a port is the difference in signal levels between the input and the isolated port when the other ports are under matched conditions. The isolation factor ($S_{23,}$ $S_{24,}$ $S_{25,}$ $S_{34,}$ $S_{35,}$ S_{45}) achieved by the novel Wilkinson Divider remains below -10dB for maximum TWI frequency range as shown in Figure 3-7.

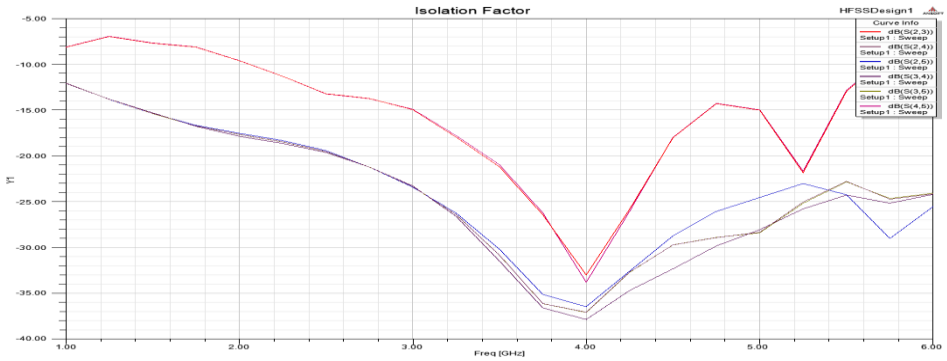

Figure 3-6 - Isolation Factor of 1-to-4 WPD

3.5.3 Phase Difference and Group Delay

Phase difference is the difference between two waves having the same frequency and referenced to the same point in time. The phase difference between the input and output ports is displayed in Figure 3-8.

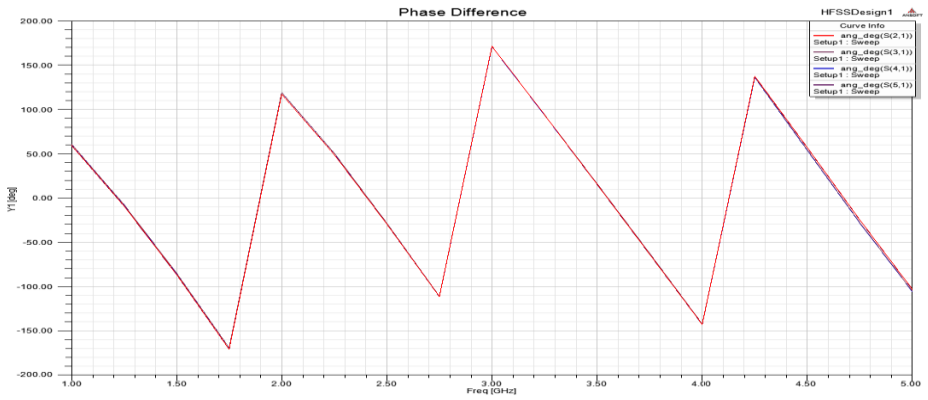

Figure 3-7 - Phase Difference of 1-to-4 WPD

The simulation results show that the phase difference oscillates between ±3 degrees as shown in Figure 3-8. However, the important thing to note is that as the phase delay encountered by all output ports is the same, therefore, the group delay encountered is non-existent. Group delay is troublesome as it causes poor fidelity and inter symbol interference. Absence of Group Delay significantly simplifies the device as no adaptive equalizers are required to compensate this delay

3.6 Summary

The power divider module focuses on the designing and development of a low cost 1-to-4 Micro-strip Wilkinson Power Divider for use in Through Wall Imaging Applications. The results show that the proposed 1-to-4 Wilkinson divider provides excellent performance characteristics with a good high conformity between the theoretical and practical results.

Chapter: 4

ANTENNA STEERING MODULE

4.1 Introduction

Amplitude and phase of reflected signal are extracted from the return loss plots. Measurements from multiple points are required for the efficient completion of the imaging process. Therefore, a positioning mechanism is required on which the antenna can be mounted and moved in an accurate and controlled fashion, as is required, for imaging process to commence. For the detection and localization of objects, a one dimensional horizontal scan is sufficient. However for working on the geometry of objects, 2D scanning is required. Hence a 2D Positioner is required that can move the antenna in both horizontal and vertical directions. The Positioner, to be used in the project, had to be designed keeping in view the requirements of the imaging process. It has to have a good precision since the precision of the imaging process depends on it. Furthermore, it has to be controllable and interface-able with computer to automate the positioning process and to accommodate for control of Positioner from within the algorithm.

4.2 Mechanism Design

One for the main goals in selection of design characteristics was to achieve a considerable measure of accuracy while keeping costs and weight at a minimum; using components easily available in the local market at an affordable price.

4.2.1 Motors

The motor had to have a good degree of precision in movement, have minimum backlash and should have had a high torque to be able to move the assembly. Availability and cost also had to be put into account. Stepper motors were considered as a first choice due to the ease of ability to control them, wherein, the motor could take control pulses directly from the control unit (e.g. microcontroller) and angular movement was also controlled and calculated.

However stepper motor as in Figure 4.2(b) was found to be unsuitable for the purpose due to their insufficient torque and excessive backlash. The option selected instead was of a servo motor as in Figure 4.2(a). It was found to have very small backlash, an in-built breaking mechanism and generated enough torque to manage the application properly.

Figure 4-1 (a) – Servo Motor

Figure 4-1 (b) – Stepper Motor

4.2.2 Need of driver stage

Servo motor being a high torque motor has high power requirements. It drew more current (typically around 2-3A). Microcontrollers provide currents usually of the order of 50mA. So an intermediate driver stage had to be made externally to drive and control these motors. H bridges using relays with considerable current ratings were used for the driver stage

4.2.3 H Bridge

An H-Bridge is an electronic circuit which can be built using discrete components. It is used to drive motors in forward and backward direction because voltage can be applied across a load in either direction.

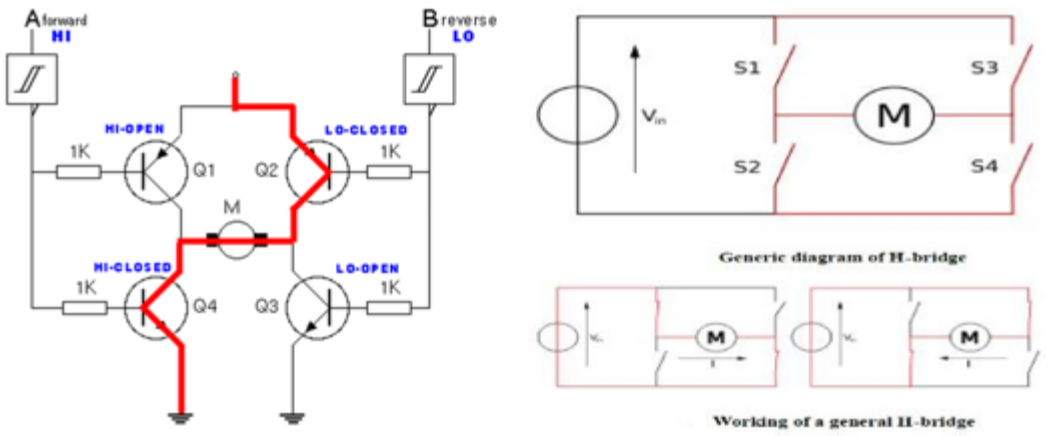

Figure 4-2 - H-Bridge Design and Operation

As shown in the Figure 4-2, H-bridge is contains four switches which can be mechanical or solid state. When the switches S1 and S4 are closed and the other two are open a positive voltage will be applied across the motor. By opening S1 and S4 switches and closing the other two switches, this voltage is reversed, allowing the motor to operate in opposite direction.

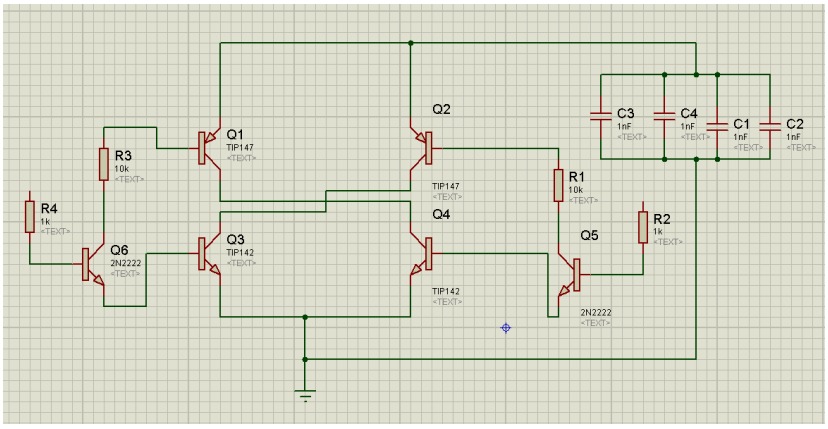

Figure 4-3 - H-Bridge Design Simulation

H- Bridge with considerable current ratings if 12A and voltage rating of 24V was used. Motion in both dimensions was achieved using two separate motors, one motor was used for the horizontal movement while the second one was used for the vertical movement.

4.3 Positioner control

4.3.1 Microcontroller

As mentioned before, one of the main tasks while designing a Positioner was to design an efficient control mechanism for the Positioner wherein, movement of the Positioner and the pattern of movement could be changed by the user according to his/her need. Using H Bridge with switching mechanism had enabled movement of both motors in both directions. Microcontrollers were used for switching. Pulses output from these microcontrollers are used to control the movement. The microcontroller used was PIC 18F452 as displayed in Figure 4-4.

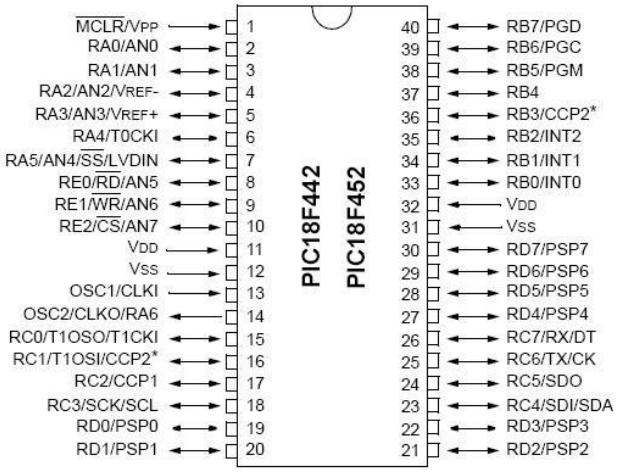

Figure 4-4 - PIC18F452 PIN Configuration

4.3.2 Positioner interface with PC

Microcontrollers are coded for control of Positioner movement. However, there is a need for controller to be interfaced with the computer so that the imaging process can be synchronized with the Positioner movement. We would ideally want to take reading from VNA when the antenna is stationary. This interface would also provide various options in control whereby certain parameters can be conveniently input from the user. For that purpose, serial port (RS-232) was chosen.

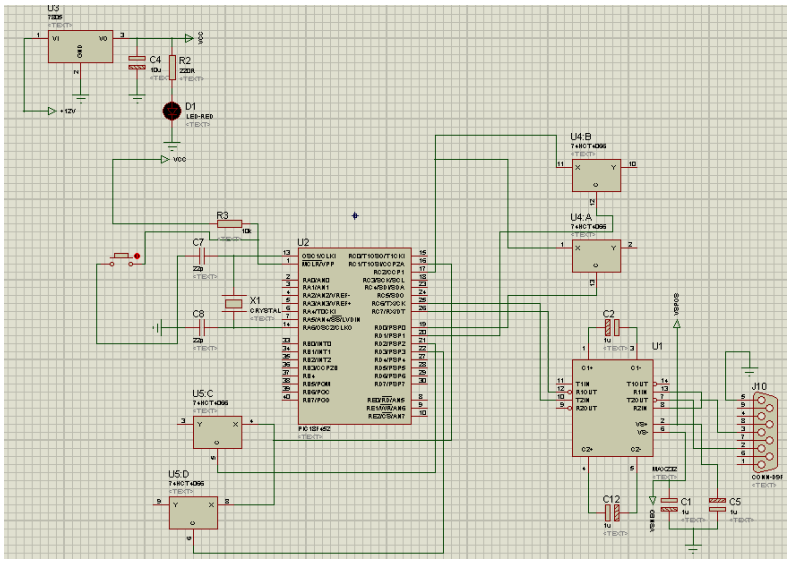

Figure 4-5 - Serial Comm. Design Simulation

A Matlab code was developed in which the user just has to enter the number of vertical and horizontal steps and the scanning is carried on automatically from there. The Positioner assembly is displayed in Figure 4.10

Figure 4-6 - Antenna Steering Mechanism

4.4 Summary

Design and development of 2D antenna positioning assembly and it automatic control using microcontrollers and various other circuitry has been explained in this chapter. The attributes (amplitude and phase) of the reflected signal are being used for through the wall imaging. An accurate result is difficult to be achieved by taking reading at a single point only. Thus there is a need to move the antenna at various positions in a controlled and calculated fashion. For this, a controllable and computer interface-able Positioner with considerable accuracy is designed and constructed. The use of H-bridge, microcontroller programming provide an effective and user friendly means of control.

Chapter: 5

FIELD RESULTS

5.1 Introduction

The field trials were carried out in a real environment with the objective of detection and localization of individual target. The different scenarios used are depicted in Figure 5-2 up to Figure 5-7.

5.2 Image Processing

Noise present in a system is reduced by comparing it with an estimation of the desired noiseless signal. Wiener filter is a type of filter which uses this principle. Based on statistics estimated from a local neighborhood of each pixel, these filter cancel noise from the signal.

5.2.1 Weiner Filter

The Wiener filter is a filter proposed by Norbert Wiener during the 1940s and published in 1949. This filter blocks the noise that has distorted the signal. It is based on a statistical approach. [30] Wiener filters are characterized by the following:

- **Assumption:** The Signal and additive noise spectral features are known and are stationary linear stochastic processes
- **Requirement:** To make the filter causal it must be physically realizable
- **Performance Criterion:** Minimum mean-square error (MMSE)

5.2.2 Wall Parameters

Wall parameters are the most important variables in through the wall imaging because they change not only with the material of the wall but also with its thickness. Design of TWI system needs the knowledge of constitutive parameters of different building materials. To find out the total one way attenuation, the results given in Figure 5-1 have been extrapolated in the frequency range of 3-6 GHz. Using the extrapolated values, the maximum attenuation has been found out to be 5 dB, in case of concrete, at 4 GHz frequency.

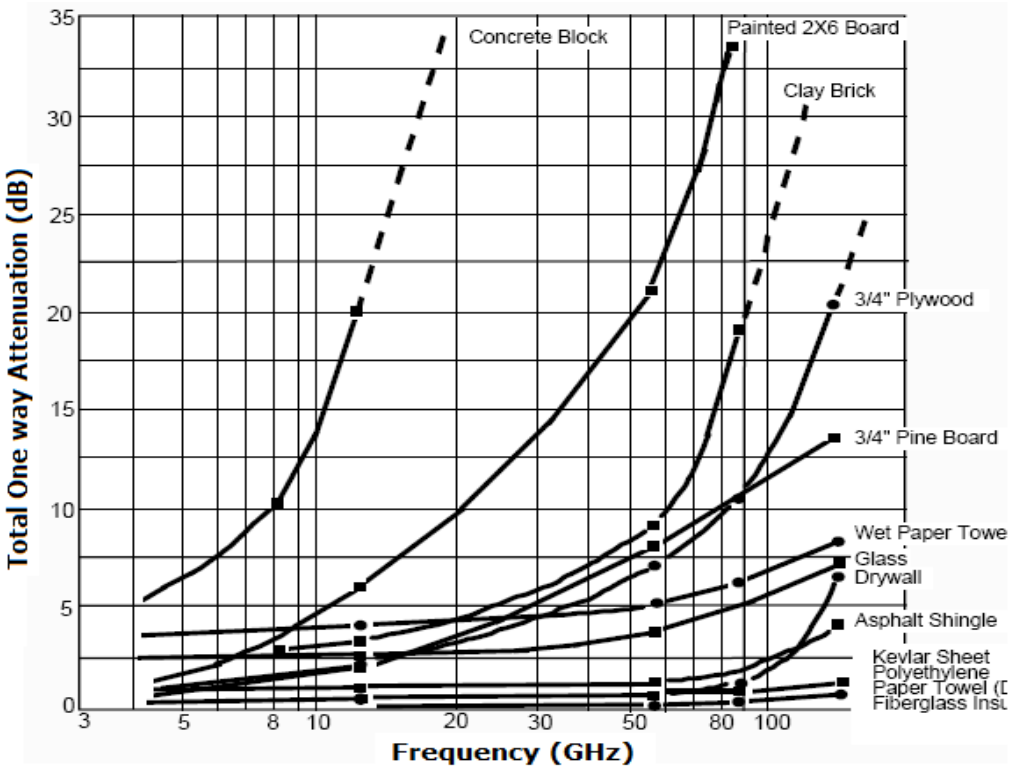

Figure 5-1 - Attenuation vs. Frequency Characteristics of Different Walls [31]

To cater for this problem, the antenna system has been designed in such a way that it produces an extra gain in excess of 5 dB to overcome this attenuation.

5.3 Scenarios and Results

5.3.1 Scenario-I: Human Target Detection across a Wooden Wall

This scenario involves human localization across a wooden wall. The human target was present at a specific location, as shown in Figure 5-2.

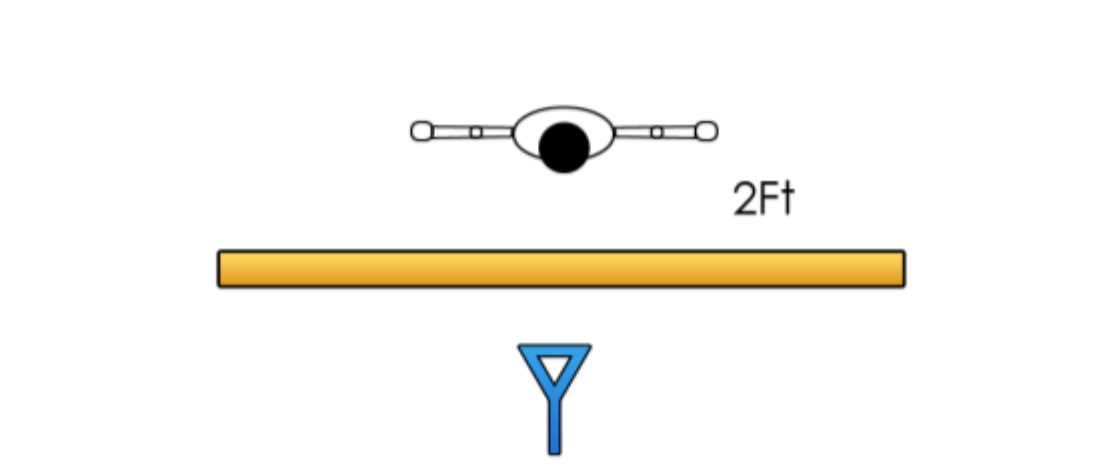

Figure 5-2 - Scenario-I: Human Target Detection across a Wooden Wall

Results

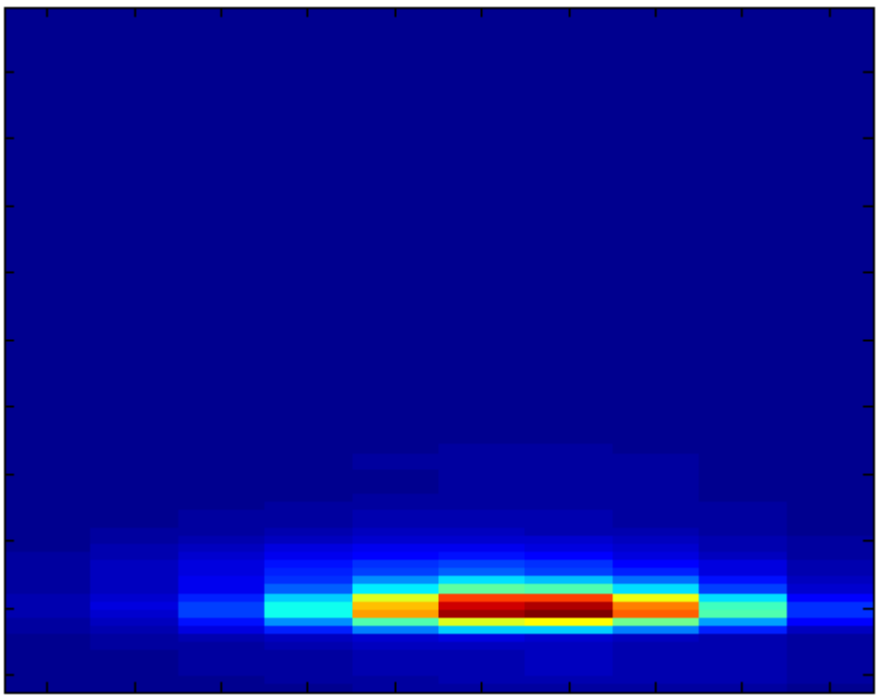

Figure 5-3 - Scenario-I Results: Human Target Detection across a Wooden Wall

5.3.2 Scenario-II: Human Target Detection across a Wooden Wall

This scenario involves the detection of a human at a distance of 4 ft. across a wooden wall, as shown in Figure 5-4 and its corresponding result in Figure 5-5.

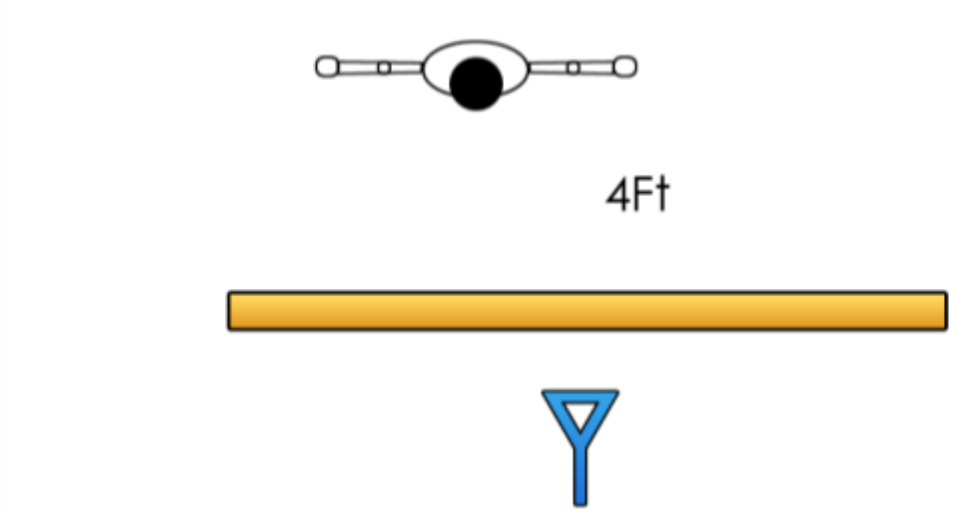

Figure 5-4 - Scenario-II: Human Target Detection across a Wooden Wall

Results

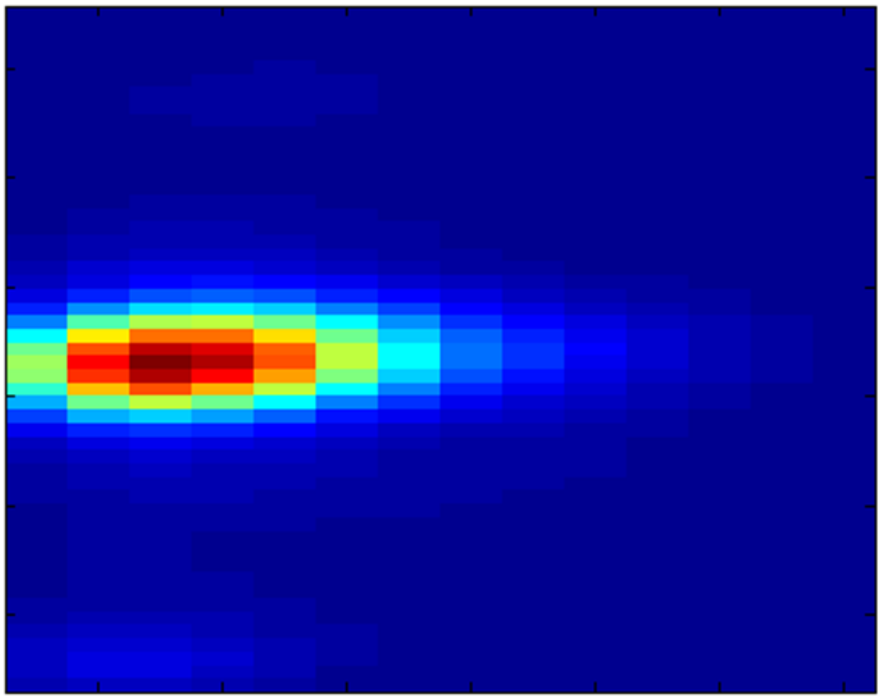

Figure 5-5 - Scenario-II Results: Human Target Detection across a Wooden Wall

5.3.3 Scenario-III: Metallic Object Detection across a Wooden Wall

This scenario involves metallic object detection, placed across a wooden wall. The target is located 3 ft. away from the wall, as indicated in Figure 5-6.

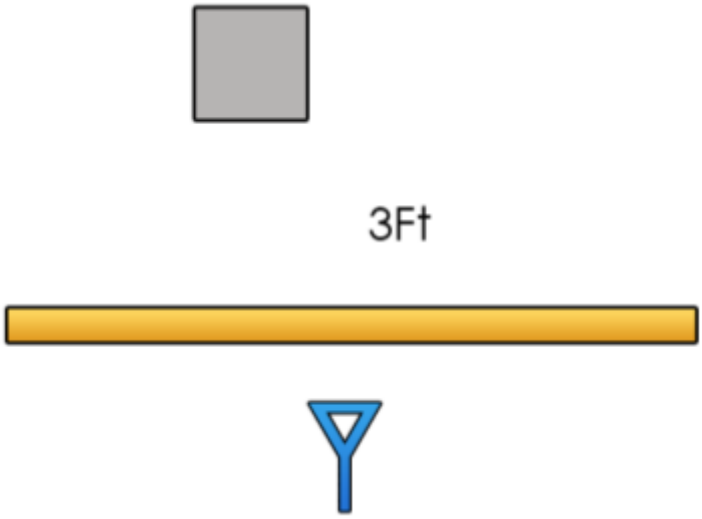

Figure 5-6 - Scenario-III: Metallic Object Detection across a Wooden Wall

Results

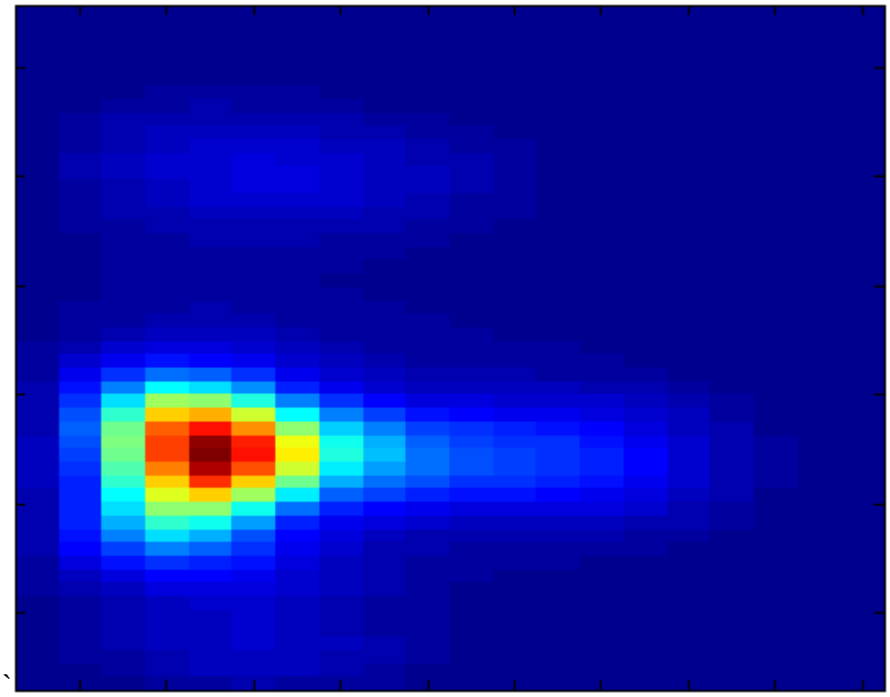

Figure 5-7 - Scenario-III Results: Metallic Object Detection across a Wooden Wall

5.3.4 Scenario-IV: Human Detection and Beam Forming across a Wooden Wall

This scenario involves human detection and 3D image formation giving details about the object geometry, placed across a wooden wall. The target is located 2 ft. away from the wall, as indicated in Figure 5-8.

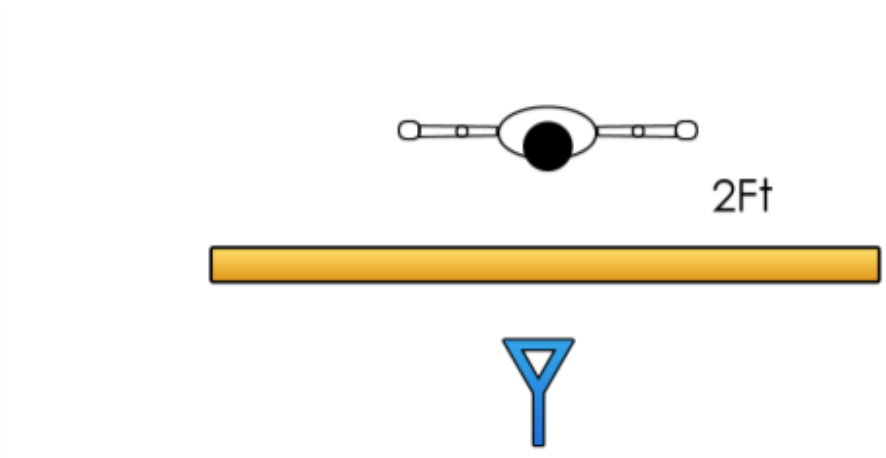

Figure 5-8 - Scenario-IV: 3D Beam-forming

Results

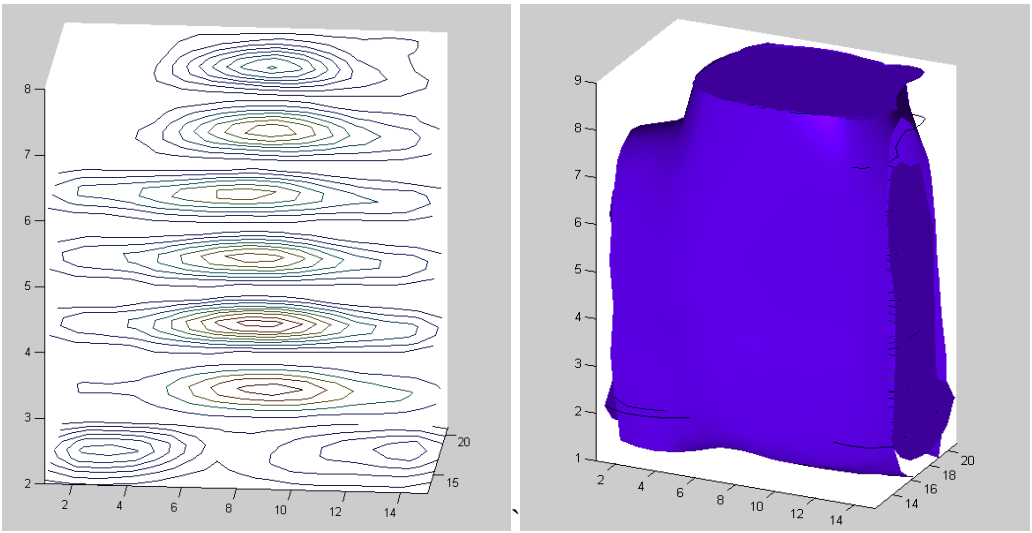

Figure 5-9 - Scenario-IV Results: 3D Beam-forming

Chapter: 6

INTEGRATED SETUP

6.1 Introduction

The integrated setup is as shown in the Figure 6-1. The data is provided by antenna system to the VNA via the power divider architecture. After conversion of data into digital form, the signal processing is delivered to the PC via a serial port or Ethernet.

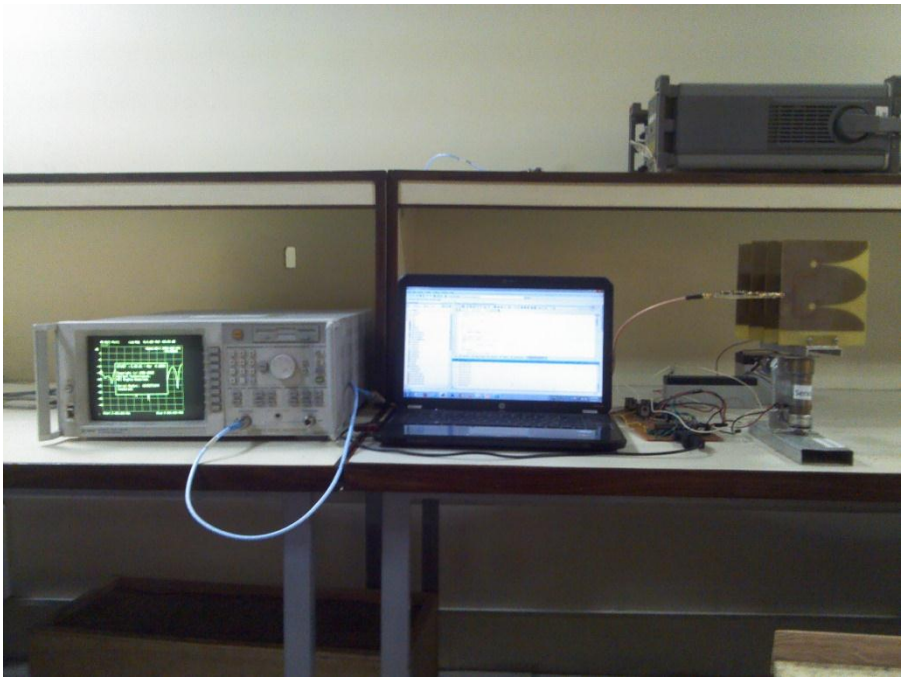

Figure 6-1 - Integrated Through-the-Wall Imaging System

6.2 Future Work

Future work involves the development of a small, dedicated and compact reflection coefficient measurement device. It would greatly make the system more cost effective because presently VNA has been used which is quite expensive. Incorporation of image processing on FPGA based architecture is another arena to explore, since it would make the system faster and more efficient.

Another area for future work involves the detection of multiple objects across multiple walls, along with their geometry and precise distance. The technology can further be improved which is capable of detecting breathing and heartbeat.

6.3 Conclusion

A prototype mobile radar microwave imaging system has been designed and built which is capable of detecting and localizing objects present behind opaque walls. The project finds its application in many crucial areas ranging from military to law enforcement and from emergency to healthcare.

APPENDICES

Appendix ‘A’

Data Collection Code

```
clear all;
close all;
%.....Running ftp protocol on vna……..

fd=ftp('192.168.1.20','network','analyzer')

%.....change directory to data folder in vna ram……..

cd(fd,'data')

%.....serial port initialize……..

s=serial('com48')
fopen(s)

N=15;                                  %.....Number of A-scans to be cascaded

for k=1:N
        tic
   mget(fd,'trace1.s1p')               %..... Retrieve .s1p touchstone file

   fwrite(s,7)                         % …….....Move antenna by 1 step
   h = read(rfdata.data, 'trace1.s1p'); %.....extract matrix from .s1p touchstone file
   [E,f] = extract(h,'S_parameters');

save(strcat('new_array_object_1',num2str(k)),'E','f');  %...save E and f for every sweep

        k
        toc
end
fclose(s)
```

2D Data Formation Code

```
%.....x-axis = horizontal scan

%.....y-axis = depth scan

%.....z-axis = vertical scan

clc; close all; clear all

N=15;                          %.....Number of scan point along x-axis

%.....With Target……..

for k=1:N

   load(strcat('new_array_object_1',num2str(9)),'E')

   object_Target(:,k)=E;

end

size(object_Target);

save object_Target object_Target


%.....Without Target…….

for k=1:N

  load(strcat('new_array_empty_0',num2str(k)),'E')

   object_Empty(:,k)=E;

end

size(object_Empty);

save object_Empty object_Empty


%.....variables…….

Ts=(1e-9)/4;

c=3.281*(3e8)/2;

z=(0:Ts:(201*4-1)*Ts).*c;
```

```
%..... Ifft……

for k=1:N
  data_Target(:,k)=ifft(object_Target(:,k),201*4);
  data_Empty(:,k)=ifft(object_Empty(:,k),201*4);
end

time_domain = data_Target - data_Empty;
save time_domain time_domain

%.....Results…….

x = 1:N;
z1 = 60;                %..... Start point of display
z2 = 80;                %……... End point of display
H = fspecial('average');
%.....Image-I……
A = abs(time_domain(z1:z2,:)).^2;
B = flipdim(A,1)       % Data alignment, so wall is at bottom of plot
X=B;
%.....Image-II……
B = wiener2(X,[2 2]);
%.....Image-III……
C = imfilter(B,H');
%.....Image-IV…….
D = wiener2(C,[5 5]);
D = imfilter(D,H');
```

```
%.....................Display of Scan……
figure(1);subplot(221);imagesc(x,z(z1:z2),C);title('Original Image')
subplot(222);imagesc(x,z(z1:z2),B);title('Wiener Image (Variance Smoothened)')
subplot(223);imagesc(x,z(z1:z2),C);title('Feature Extraction')
subplot(224);imagesc(x,z(z1:z2),D);title('Smoothened Image')
hold on
save(strcat('time_domain_',num2str(j)),'C')  ; %..... j=scan number along z-axis
```

Appendix ‘C’

3D Data Formation Code

```
N=8;                    %..... number of layers along z-axis
for k=1:N
   load(strcat('time_domain_',num2str(k)),'C')
a=size(C);              %..... To get dimensions of scanned image
b=(max(max(C)))/10; %..... Maximum value in scan (to discard unnecessary values)
x=1;y=1;z=0;
        while(x<=a(1,1))

                while(y<=a(1,2))
                        z=C(x,y);
                         if(z<b)
                        C(x,y)=0;       %..... Unnecessary values get replaced by zero
                        end
                        if(z>b)
                        C(x,y)=z*1500000;  %..... Desired values get scaled
                         end
                y=y+1;
                end
        x=x+1;
        y=1;
        end
variable(:,:,k)=C;                      % …....3D Variable
end
save TWI variable
```

```
%.....load 3D Variable Data……..
load TWI
D=variable;
%.....Displaying 3-D Contour Slices……

phandles = contourslice(D,[],[],[1,2,3,4,5,6,7,8]);
view(3); axis tight
set(phandles,'LineWidth',1)

%.....Displaying an Isosurface…….

Ds = smooth3(D);
hiso = patch(isosurface(Ds,5),...
        'FaceColor',[0.4,0,1],...
        'EdgeColor','none');
%.....Adding an Isocap to Show a Cutaway Surface…….

hcap = patch(isocaps(D,4),...
        'FaceColor',[0.4,0,1],...
        'EdgeColor','none');

%.....Defining the View……

view(30,45)
axis tight
daspect([1,1,.4])

%.....Add Lighting……..

lightangle(0,0);
set(gcf,'Renderer','zbuffer'); lighting phong
isonormals(Ds,hiso)
set(hiso,'SpecularColorReflectance',0,'SpecularExponent',50)
set(hcap,'AmbientStrength',.6)
```

Appendix ‘D’

User Guide

Objective:

- To detect and localize the targets present behind the wall using TWI System.

Equipment:

- 1 x Agilent 8417ET VNA for 300kHz-3GHz
- 1 x VNA Calibration Kit
- 4 x Vivaldi Array Antenna
- 1 x Wilkinson Power Divider
- 1 x N Male to N Male RF Cable
- 2 x SMA Male to SMA Male RF Cable
- 1 x SMA Male to N Female RF Converter

Installation and Operation:

- Power on the Computer Work station.
- Plug in the Vector Network Analyzer (VNA) and turn it ON.
- Follow the following steps to establish connection between VNA and PC using a LAN cable:
    - Assign IP address 192.168.10.20 to VNA
    - Assign default gateway 192.168.10.100 to VNA and PC
    - Assign IP address 192.168.10.10 to PC
    - Restart the PC
- Mount the Antenna Array Antennas.
- Connect the Array Antennas to the output terminals of the Wilkinson Power Divider via the two SMA Male to SMA Male RF Cables.
- Calibrate the VNA using the steps mentioned below:
    - Connect one end of the N Male to N Male RF Cable to the VNA.
    - Press the CAL button on the VNA Screen
    - Connect SHORT to other end of RF Cable and press MEASURE STANDARD button.

    - Connect OPEN to RF cable and press MEASURE STANDARD button
    - Finally connect LOAD to RF cable and press MEASURE STANDARD button.
    - Now the VNA is calibrated.
- Connect the SMA Male to N Female RF Converter to the other end of the N Male to N Male RF Cable to make it an N Male to SMA Male RF Cable.
- Connect the input terminal of the Wilkinson Power Divider with the calibrated Vector Network Analyzer by means of the N Male to SMA Male RF Cable.
- Adjust the VNA settings in order to record S_{11}.
    - Set the power to 19.99 dBm
    - Set the start frequency range to 3000MHz
    - Set the stop frequency range to 6000MHz
    - Set the number of sweep points to 201
    - In the parameter settings, choose the REFLECTION option
    - Change the display format to LOG MAGNITUDE
- Connect the Vector Network Analyzer to the Computer via a LAN cable.
- Run the Data Collection MATLAB code to collect the TWI data.
- Afterwards, run the Data Formation MATLAB Code.
- After the acquisition of scan data, the code will automatically display the TWI results in form of an intensity plot.

Precautions:

- Do not keep the power level of VNA too high.
- Do not touch the metallic layers of the Array Antennas and Wilkinson Power Divider.
- Do not bend the RF cables.
- Do not use long lengths of RF cables.
- Turn OFF power of VNA after completing the experiment.

Trouble Shooting:

- VNA is not working
    - Check whether the VNA switch is properly plugged into the socket.
    - Check the availability of electricity.
- MATLAB Code not running
    - Check whether the LAN Cable is connected properly.
    - Check whether the VNA and Computer have appropriate IP address and Gateway settings.
    - Check whether the code files are placed in the active MATLAB directory.
- Results are not obtained
    - Check if the VNA is calibrated.
    - Check whether the IP address and Gateway settings in the code files are set properly.
    - Check whether the output variables are the same in both the codes.

BIBLIOGRAPHY

BIBLIOGRAPHY

[1] Sisma, Ondrej, Alain Gaugue, Christophe Liebe, and Jean Marc Ogier. "UWB Radar: Vision through a Wall." Telecommunication Systems Journal (Springer), 2008: 53-59.

[2] Camero - Step into the known: Life Saving Applications. http://www.camero-tech.com/applications.shtml (accessed July 1, 2010).

[3] Aftanas, Michal. "Through Wall Imaging With UWB Radar System." PhD Thesis, Department of Electronics and Multimedia Communications, Technical University Of Kosice, 2009.

[4] Chen, F.C., Chew, W.C. "Time-Domain Ultra-Wideband Microwave Imaging Radar System." IEEE Instrumentation and Measurements Technology Conference. IMTC/98. 1998.

[5] Bowick, Christopher, John Blyler, and Cheryl Ajluni. RF Circuit Design. 2nd Edition. Newnes, Elsevier, 2008.

[6] Center for Advanced Communication: Experiments On Through-The-Wall Imaging. http://www.villanova.edu/engineering/centers/cac/twri.htm (accessed July 2, 2010).

[7] Baranoski, Edward J. "Through wall imaging: Historical perspective and future directions." ICASSP 2008. DARPA, 2008. 5173-5176.

[8] Dahl, Øyvind. "High-precision Beamforming with UWB Impulse Radar." MS Thesis. University of Oslo, April 1, 2009. 92.

[9] Yang, Y., Y. Wang, and A. E. Fathy. "Design of Compact Vivaldi Antenna Arrays for UWB See Through Wall Applications." Progress In Electromagnetics Research, PIER-82, 2008: 401–418.

[10] Scholtz, Robert A., David M. Pozar, and Namgoong Won. "Ultra-Wideband Radio." EURASIP Journal on Applied Signal Processing (Hindawi Publishing Corporation), 2005: 252-272.

[11] Gibson, P. J. "The Vivaldi Aerial." European Microwave Conference: 9th Proceedings, June 1979.

[12] Rajaraman, Raviprakash. "Design of a Wideband Vivaldi Antenna Array for the Snow Radar." MS Thesis. Lawrence, Kansas: University of Kansas, February 2004.

[13] Panzer, Ben. "Development of an Electrically Small Vivaldi Antenna: The Cresis Aerial Vivaldi." MS Thesis. Lawrence, Kansas: University of Kansas, 2004.

[14] Chen, Fang. "MS Thesis." Design, An Improved Wideband Vivaldi Antenna. Edinburg, Texas: University of Texas Pan-American May 2010.

[15] Oraizi, Homayoon, and Jam Shahrokh. "Optimum Design of Tapered Slot Antenna Profile." IEEE Transactions on Antennas and Propogation 51, no. 8 (August 2003).

[16] Balanis, Constatine A. Antenna Theory: Analysis and Design. 2nd Edition. Singapore: John Willey & Sons, Inc., 2005.

[17] Pozar, David M. Microwave Engineering. 3rd Edition. Jonh Wiley & Sons, 1997.

[18] Nevrly, Josef. "Design of Vivaldi Antenna." Diploma Thesis. Prague: Czech Technical University, 2007.

[19] Yngvesson, K. S., T. L. Korzeniowski, Y. S. Kim, E. L. Kollberg, and J. F. Johansson. "The Tapered Slot Antenna - A New Integrated Element for Milimeter-wave Applications." IEEE Transactions on Microwave Theory and Techniques, 1989: 365-374.

[20] Johnsson, R.C. Antenna Engineering Handbook. McGraw-Hill, 1993.

[21] Desmond, Chee Tiong. "Smart Antennas for Wireless Applications and Switched Beamforming." BE (Bachelor of Engineering) Thesis. Brisbane: University of Queensland, October 2001.

[22] Wilkinson Power Splitters. October 2010. http://www.microwaves101.com/encyclopedia/Wilkinson_splitters.cfm (accessed May 2011).

[23] Sebak, A. R. "A Modified Wilkinson Power Divider/Combiner for Ultrawideband Communications." IEEE, 1-4: 2009.

[24] Shamsinejad, S., M. Soleiman, and N. Komjani. "Novel Miniaturized Wilkinson Power Divider for 3G Mobile Receivers." IEEE, 2008: 1-3.

[25] Wolff, Christian. Radar Basics - Phase Array Antenna. March 29, 2011. http://www.radartutorial.eu/06.antennas/an14.en.html (accessed April 10, 2011).

[26] John Wiley & Sons, Inc. Thomas Young. 1998. http://web.sbu.edu/chemistry/wier/electrons/young.html (accessed April 12, 2011).

[27] Wolff, Christian. Radar Basics - Phase Shifter for Phased Array Antennae. March 29, 2011. http://www.radartutorial.eu/06.antennas/an16.en.html (accessed April 10, 2011).

[28] Wikipedia, the free encyclopedia. PIN Diode. April 2011. http://en.wikipedia.org/wiki/PIN_diode.

[29] Wolff, Christian. Radar Basics - PIN Diodes. http://www.radartutorial.eu/21.semiconductors/hl14.en.html (accessed April 11, 2011).

[30] Wikipedia, the free encyclopedia. Wiener Filter. April 2011. http://en.wikipedia.org/wiki/Wiener_filter.

[31] Kapilevich, B., M. Einat, A. Yahalom, M. Kanter, B. Litv, and A. Gover. "Millimeter Waves Sensing Behind Walls – Feasibility Study with FEL Radiation." Edited by Israel Tel Aviv University. 29th International Free Electron Laser Conference, FEL 2007. Novosibirsk, Russia, 2007. 501-504.